Time resolved four- and six-wave mixing in liquids. I. Theory

Steffen, T.; Fourkas, J. T.; Duppen, K.

Published in:
Journal of Chemical Physics

DOI:
10.1063/1.472594

Time resolved four- and six-wave mixing in liquids. I. Theory

Thomas Steffen, John T. Fourkas, and Koos Duppen

Citation: The Journal of Chemical Physics **105**, 7364 (1996); doi: 10.1063/1.472594
View online: https://doi.org/10.1063/1.472594
View Table of Contents: http://aip.scitation.org/toc/jcp/105/17
Published by the American Institute of Physics

Time resolved four- and six-wave mixing in liquids. I. Theory

Thomas Steffen
Ultrafast Laser and Spectroscopy Laboratory, Department of Chemical Physics, Materials Science Center, University of Groningen, 9747 AG, The Netherlands

John T. Fourkas
Eugene F. Merkert Chemistry Center, Boston College, Chesnut Hill, Massachusetts 02167

Koos Duppen
Ultrafast Laser and Spectroscopy Laboratory, Department of Chemical Physics, Materials Science Center, University of Groningen, 9747 AG, The Netherlands

(Received 16 April 1996; accepted 12 July 1996)

Low-frequency intermolecular dynamics in liquids is studied by ultrafast four- and six-wave mixing. The theory of these nonlinear optical processes is given for electronically nonresonant optical interactions up to fifth order in the electric field. The Born–Oppenheimer approximation is used to separate the motional part of the response functions from coordinate independent electronic hyperpolarizabilities. A large variety of experiments, involving far-infrared absorption, ordinary Rayleigh–Raman or hyper Rayleigh–Raman scattering is covered by this theory. The response in nonresonant six-wave mixing comprises four dynamically different processes. It is shown that one of the terms contains information on the time scale(s) of intermolecular dynamics, that is not available from lower-order nonresonant experiments. For instance, homogenous and inhomogeneous contributions to line broadening can be distinguished. The optical response of harmonic nuclear motion is calculated for nonlinear coordinate dependence of the polarizabilities. Results for level-dependent and level-independent damping of the motion are compared. It is shown that level-dependent damping destroys the interference between different quantum mechanical pathways, yielding an extra contribution to the fifth-order response that has not been discussed before. When two or more nuclear modes determine the optical response, their relative contributions to the four- and six-wave mixing signals are in general different. These contributions are determined by the coordinate dependence of the electronic polarizability, which is usually not fully known. Model calculations are presented for the dynamic parameters of liquid CS_2. The theory of this paper will be employed in Part II, to analyze experimental results on femtosecond four- and six-wave mixing. [S0021-9606(96)51439-X]

I. INTRODUCTION

A vast range of physical, chemical, and biological phenomena occurs preferentially or even exclusively in a liquid environment, due to the fact that the motions of the solvent molecules provide a very efficient heat bath for internal degrees of freedom of the solute. This heat bath is responsible for fluctuations in the structures and energy levels of molecules, and promotes or hinders thermally activated processes in these systems. Understanding the motions of the heat bath is therefore crucial for a comprehensive description of the underlying microscopic processes.[1,2] This is a complex problem, since the molecules exhibit strong mutual interactions in rapidly changing configurations. Even on a local scale, structural order exists only for short times, because of the random thermal motion of the molecules. Despite many years of experimental and theoretical effort, the microscopic aspects of low-frequency motions in liquids are still poorly understood. The lack of understanding is partly due to the limited information content of conventional experimental techniques, as well as to unwarranted simplifying assumptions for potentials, employed in molecular dynamics simulations.

Traditionally, the dynamics of atomic and molecular liquids are studied by far-infrared (FIR) absorption spectroscopy[3,4] or by Rayleigh–Raman scattering,[5–8] that measure the Fourier transform of the one-time correlation function of the dipole moment and polarizability, respectively. In the thermal range below 300 cm^{-1}, the fluctuations in these bulk properties are associated with the same low-frequency intermolecular motions. However, a unified microscopic description of the results from these experiments is rather complicated, since the different nuclear modes change the dipole moment and the polarizability in different ways. In particular, the part of the response that is due to many-body effects, i.e., interaction-induced changes of the dipole moment and polarizability, is based on different mechanisms.

In the last decade, the conventional techniques have been supplemented by a variety of stimulated time- and frequency-domain light scattering experiments. Examples in frequency domain are stimulated gain spectroscopy (SGS),[9,10] tunable laser-induced gratings (TLIG),[11] and stimulated Rayleigh-wing spectroscopy (SRWS).[12,13] Most time-domain experiments are based on impulsive stimulated

scattering, initiated by femtosecond pulses,[14–17] but experiments using the short correlation time of incoherent light have also been reported.[18] All Raman-active modes within the large spectral width of a short pulse, i.e., that have a period longer than the pulse duration, are excited impulsively. Two configurations are used for time-resolved measurements of low-frequency dynamics: In optical Kerr effect (OKE) experiments a strong, polarized pump pulse induces transient birefringence in the originally isotropic liquid, that causes a polarization rotation of a weak delayed probe pulse.[19–26] In transient grating scattering (TGS) two interfering pulses induce a spatially modulated index grating in the liquid that scatters a variably delayed probe pulse in the Bragg direction.[27–32]

It has been shown theoretically[33] and experimentally[34–36] that the spontaneous and stimulated frequency- and time-domain light scattering methods, discussed so far, have in principle an equivalent information content and are related by Fourier transformation, independent of any dynamical model. The basic physics can be expressed equally well by time-domain response functions or by frequency-domain susceptibilities. In practice the choice of the particular experimental technique will be determined by technical considerations. Compared to spontaneous scattering, the stimulated techniques have the advantage that the high-frequency components are not underestimated, since the response is directly proportional to the susceptibility or response function. The main advantage of time- over frequency-domain methods is that the difference between an exponential decay and an overdamped oscillation, exhibiting a distinct inertia-limited rise time, shows up more clearly in time domain.[27] In frequency domain, this information is contained in the weak far wings of the spectral response. Optical heterodyning, that was incorporated in the optical Kerr effect,[20,21] transient grating scattering,[32] and stimulated gain spectroscopy,[9,10] allows one to measure the in- and out-of-phase part of the material response separately, avoiding cross terms between them.

The general picture that emerged from both frequency- and time-domain work on intermolecular motions in liquids is well-established: The optical field exerts a torque on the molecules via the single-molecule dipole moment or the anisotropic part of the polarizability (essentially rotation absorption and rotation-Raman scattering). Additionally, all liquids, even those consisting of nonpolar and isotropically polarizable atoms or molecules, show a collective optical response of dimers, trimers, and higher aggregates, which is often referred to as the collision- or interaction-induced response.[37–39] The short-time (high-frequency) part of the response is inertial, i.e., due to their finite moment of inertia the molecules cannot follow the optical excitation instantaneously.[20,27] For highly polarizable anisotropic molecules like carbon disulfide (CS_2) and benzene, the inertial response is attributed mainly to coherent librations. Both the local equilibrium position and the librational frequency are determined by the transient local cage structure, formed by the neighboring molecules. Upon excitation of the libration the cage is distorted and the molecule acquires a new equilibrium position. The long-time (low-frequency) part of the subsequent optical response arises from diffusive reorientation of the molecules, which can be described by conventional Debye theory.[40,41]

In the itinerant oscillator model of liquid dynamics, initially developed for the explanation of FIR absorption spectra,[42–45] the single-molecule and the cage motion are projected onto two coupled harmonic modes. Most results of stimulated scattering experiments were analyzed by a simpler model, that neglects this coupling. The ultrafast coherent librations are then described by an underdamped harmonic mode, while the slow incoherent diffusion is treated as an independent heavily overdamped harmonic mode. In the instantaneous normal-mode model of liquid dynamics, single-molecule and cage motions are not identified as separate processes. Instead, the excitations are considered to be collective motions of many molecules,[46–49] similar to phonons in translationally invariant solids. For some systems it was shown that the frequency distribution of normal modes resembles the spectral density of coherent oscillations, as determined from time- or frequency-domain experiments.[50,51] This seems to indicate that the optical coupling constants do not depend on the frequency of such modes, and that the liquid is, to a good approximation, static on the time scale of the inverse frequencies of these modes.

An aspect that cannot be ignored in a description of liquid state dynamics is the effect of damping processes on the optical response. Due to the strong, random interactions, dephasing can be expected to contribute significantly to the spectral width. One major motivation of current research is to elucidate the nature and mechanisms of such processes, since they directly reflect the complex microscopic dynamics in the liquid. Traditionally, dephasing processes are classified as homogeneous or inhomogeneous. The latter is due to a static distribution of local environments of molecules, that do not change on the time scale of the experiment, while homogeneous broadening is caused by fast fluctuations, that change the local environment on a time scale much faster than the inverse width of the frequency response. Since nuclear motions in liquids occur over a wide range of time scales, the separation into ''fast'' and ''slow'' fluctuations is questionable, and hence it is not clear whether it is fruitful to discuss the optical response in terms of homogeneous and inhomogeneous broadening.[52–54]

In order to clarify these open questions concerning the optical response of liquids and its interpretation in terms of liquid state dynamics, the predictions of different models have to be compared to experimental results. Unfortunately, FIR-absorption spectra and time- and frequency-domain Rayleigh/Raman experiments provide information only on the total spectral response of motional degrees of freedom in liquids. They do not allow for an assessment of the dynamics that underlies such spectra, although one might hope to gain some understanding from a systematic study of spectra as a function of some external parameter (temperature, pressure, composition of the liquid, etc.). These experiments contain

only limited information, because they all depend on a single-time correlation function or its Fourier transform.[55,56] To unequivocally establish the time scale(s) of dynamics that give rise to a spectrum, multitime techniques should be employed, which implies higher-order nonlinear optical techniques. Examples of such type of experiments are resonant four-wave mixing in the IR and the Raman echo, a seventh-order nonlinear effect. They were used to study intramolecular vibrations of molecules in liquids, glasses, and solids.[57–64] In these studies the laser pulses were much longer than the vibrational periods, so the vibrational motion itself could not be resolved. On intermolecular motion, such experiments have not yet been performed.

A few years ago, Tanimura and Mukamel proposed a new fifth-order nonlinear optical technique to gain further insight into the time scales of intermolecular dynamics in liquids.[65] The theory for this effect was originally based on quantum path-integral techniques,[66,67] that allows for a Brownian oscillator description of the heat bath. Later, it was extended to classical oscillators and phonons,[68] and evaluated in a coherent state representation.[69] We will describe it here in a perturbative treatment that makes explicit use of the Born–Oppenheimer approximation, following the formalism of Hellwarth.[33] Damping will be modeled by state-dependent dephasing in the limit of weak system–bath coupling. This treatment yields the full description of nonresonant optical response up to fifth order, and comprises processes involving instantaneous four- and six-photon scattering, that have not been discussed before. The different processes carry distinctly different dynamical information, which may cause serious difficulties for the interpretation of experimental results. Our final results will be compared to existing theory[65,68,69] that avoids the weak coupling limit, but does not account for the state dependence of the damping rates.

First results of time-domain fifth-order experiments were recently reported by Tominaga and Yoshihara[70–73] and by ourselves.[74,75] Surprisingly, the results of these two groups differ in a number of important aspects, even when the same sample was investigated. For pure liquid CS_2, Tominaga and Yoshihara concluded that the theory of Tanimura and Mukamel[65] explains their data very well for mainly homogeneous broadening.[73] In contrast to this, we found for CS_2 and for some other liquids, that the theory fails to describe the full temporally two-dimensional information content of our data.[75] Possible reasons for the discrepancies will be discussed in Part II of this work, where experimental results of four- and six-wave mixing will be discussed in light of the theory presented here.[76]

In the presence of more than one dynamical mode, there is no direct way to predict the six-wave mixing result from a lower-order response, even when the dephasing mechanisms of the modes are known. The reason is that the nuclear coordinate dependence of the electronic polarizability, which determines the Raman cross sections in all orders, is in general unknown. The different modes will therefore have different relative contributions in the various orders of nonlinear response. Only in the case that the coordinate dependence of the polarizability is known for all modes, clear predictions can be made. Originally, Tanimura and Mukamel calculated the nonlinear response for exponential coordinate dependence, since this allows one to generate the response for any coordinate dependence, using the appropriate derivatives of the Liouville space generating functions.[65] The exponential form was also subsequently adopted to simulate the higher-order nonlinear response of water,[77] and used to fit experimental results.[70,72] However, it is physically unrealistic to assume that all modes obey the same coordinate dependence, especially when the modes describe phenomena of a completely different nature, such as coherent librations and diffusive reorientation.

The paper is organized as follows: In Sec. II, the perturbative treatment of nonlinear optics is reviewed, using the Born–Oppenheimer approximation and assuming that all optical fields are far below electronic resonances. Subsequently, in Sec. III the third- and fifth-order response functions of a damped harmonic mode is worked out. Model calculations are presented to show that the information content of six-wave mixing surpasses that of conventional four-wave mixing experiments. Finally, in Sec. IV the results are summarized and conclusions are drawn with respect to application of the theory to the analysis of experimental results.

II. NONLINEAR OPTICS WITHIN THE BORN–OPPENHEIMER APPROXIMATION

This section contains some aspects of nonlinear optical response theory. One conclusion will be that there are, in principle, more contributions to the fifth-order response than previously considered in literature.[65,68–73,77] The different processes carry different dynamical information which may affect the interpretation of experimental results. The perturbation treatment of nonlinear optics is briefly reviewed in Sec. II A. The results are valid under a large number of circumstances, e.g., for resonant and nonresonant radiation, and for coordinate dependent coupling between matter and radiation (non-Condon effects). In Sec. II B, the nonlinear optical response for electronically nonresonant radiation is calculated, following the model of Hellwarth.[33] The Born–Oppenheimer approximation (BOA) yields a reduced description of the nuclear dynamics in the electronic ground state, where the electrons are taken into account implicitly by an effective potential among the nuclei. The coupling between radiation and matter is then given by effective coupling constants: the electronic (hyper-) polarizabilities.

The third-order nonlinear optical response within the BOA is calculated in Sec. II C. It describes, for instance, various forms of Rayleigh/Raman scattering, and FIR four-wave mixing processes, where the applied fields are resonant with nuclear degrees of freedom. The fifth-order nonlinear response function in the BOA is derived in Sec. II D. In its

most general form it consists of 32 different contributions, given in Appendix A. When the applied optical frequencies are far above the nuclear resonances, only 4 of these 32 processes have to be considered.

A. Perturbation theory of nonlinear optical response

In a perturbative treatment of nonlinear optics the polarization created by an applied optical field is usually expanded in powers of that field

$$\mathbf{P}(t)=\mathbf{P}^{(0)}(t)+\mathbf{P}^{(1)}(t)+\mathbf{P}^{(2)}(t)+\mathbf{P}^{(3)}(t)+\cdots. \tag{1}$$

Here, $\mathbf{P}^{(n)}$ depends on the nth power of the electric field. The spatial dependence of the polarization, that leads to phase matching conditions, is suppressed. In media with inversion symmetry, and in particular in isotropic media like liquids, the polarizations depending on even powers of the electric field, $\mathbf{P}^{(0)}(t)$, $\mathbf{P}^{(2)}(t)$, and so on, vanish. Therefore we treat here only linear, third-, and fifth-order polarizations. The polarization at time t depends on the electric fields applied at all earlier times

$$P_i^{(1)}(t)=\int_{-\infty}^{\infty} dt_1 R_{ij}^{(1)}(t,t_1)E_j(t_1), \tag{2a}$$

$$P_i^{(3)}(t)=\int_{-\infty}^{\infty} dt_1 \int_{-\infty}^{\infty} dt_2 \int_{-\infty}^{\infty} dt_3 \times R_{ijkl}^{(3)}(t,t_1,t_2,t_3)E_j(t_1)E_k(t_2)E_l(t_3), \tag{2b}$$

$$P_i^{(5)}(t)=\int_{-\infty}^{\infty} dt_1 \int_{-\infty}^{\infty} dt_2 \int_{-\infty}^{\infty} dt_3 \int_{-\infty}^{\infty} dt_4 \int_{-\infty}^{\infty} dt_5 \times R_{ijklmn}^{(5)}(t,t_1,t_2,t_3,t_4,t_5)E_j(t_1) \times E_k(t_2)E_l(t_3)E_m(t_4)E_n(t_5). \tag{2c}$$

The nth order time-domain response function $R^{(n)}$ is a tensor of rank $n+1$. We use the convention that repeated space indices in a product are to be summed over. The last interaction with field E_j occurs at time t_1, the second to last interaction with field E_k at time t_2, and so on. This is shown schematically in Fig. 1(a) up to fifth order. For first- and third-order response the number of interactions has to be reduced correspondingly.

The optical field couples with the medium via the time-dependent microscopic charge distribution. In the Heisenberg picture, the polarization $\mathbf{P}(t)$ is given by the expectation value of the dipole operator $\mathbf{p}$

$$\mathbf{P}(t)=\langle U^{-1}(t)\mathbf{p}U(t)\rangle. \tag{3}$$

Here, $\mathbf{p}$ is the total dipole moment associated with the instantaneous positions of all charged particles α (nuclei and electrons):

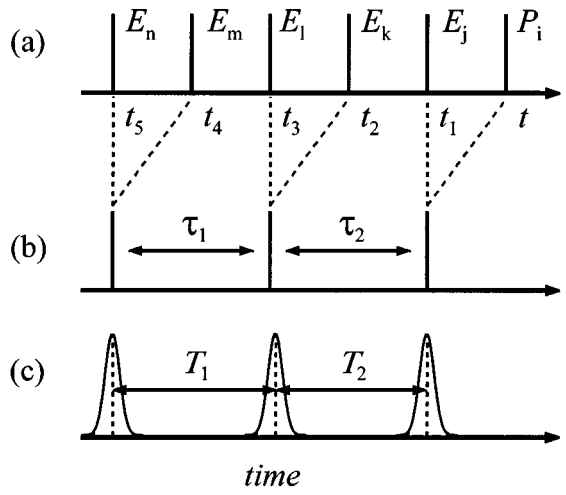

FIG. 1. Definition of the time variables as used in this paper. In (a) the five time variables t_1–t_5 are shown, denoting the times when the fields E_j–E_n act on the system to generate a nonlinear polarization P_i at time t. In (b) it is shown that $t=t_1$, $t_2=t_3$, and $t_4=t_5$ is a necessary condition for nonresonant excitation. The nonlinear response functions will be expressed in terms of the time differences $\tau_1\equiv t_3-t_4$ and $\tau_2\equiv t_1-t_2$. In third-order scattering there is only one propagation period $\tau_1\equiv t_1-t_2$. In (c) the experimental situation for six-wave mixing is depicted. Two pairs of excitation pulses, separated by time T_1, are followed by a probe pulse with delay T_2. For finite pulse durations, a range of time differences τ_1 and τ_2 occurs.

$$\mathbf{p}=\sum_{\alpha} e_{\alpha}\mathbf{r}_{\alpha}, \tag{4}$$

and $U(t)$ is the time evolution operator that satisfies

$$i\hbar \frac{dU}{dt}=(H_0+H_I(t))U. \tag{5}$$

H_0 is the Hamiltonian of the unperturbed system and H_1 is the interaction Hamiltonian, that in the electric dipole approximation is given by:

$$H_I(t)=-\mathbf{p}\cdot\mathbf{E}(t). \tag{6}$$

The polarization [Eq. (3)] can be evaluated to arbitrary order in the applied field $E(t)$ by expanding $U^{-1}(t)$ and $U(t)$ in powers of $H_I(t)$, using standard iteration techniques.[33,78,79] We do not repeat the derivations here, but only quote the main result for the dipole operator in the Heisenberg picture

$$U^{-1}(t)p_iU(t) =\tilde{p}_i(t)+\left(\frac{-i}{\hbar}\right)\int_{-\infty}^{t} dt_1[\tilde{p}_i(t),\tilde{H}_I(t_1)] +\left(\frac{-i}{\hbar}\right)^2\int_{-\infty}^{t} dt_1\int_{-\infty}^{t_1} dt_2[[\tilde{p}_i(t),\tilde{H}_I(t_1)],\tilde{H}_I(t_2)] +\cdots. \tag{7}$$

Here $[A,B]=AB-BA$ denotes a commutator and $\tilde{A}(t)$ means that the operator A is transformed to the interaction picture

$$\tilde{A}(t)=U_0^{-1}(t)AU_0(t), \tag{8}$$

where $U_0(t)=\exp(-iH_0t/\hbar)$ is the time evolution operator of the unperturbed system. Comparing Eqs. (7) and (6) with Eqs. (2), the time domain (non-) linear response functions are obtained

$$R_{ij}^{(1)}(t,t_1)=\frac{i}{\hbar}\langle[\tilde{p}_i(t),\tilde{p}_j(t_1)]\rangle H(t-t_1), \tag{9a}$$

$$R_{ijkl}^{(3)}(t,t_1,t_2,t_3)=\left(\frac{i}{\hbar}\right)^3\langle[[[\tilde{p}_i(t),\tilde{p}_j(t_1)],\tilde{p}_k(t_2)],\tilde{p}_l(t_3)]\rangle \times H(t-t_1)H(t_1-t_2)H(t_2-t_3), \tag{9b}$$

$$R_{ijklmn}^{(5)}(t,t_1,t_2,t_3,t_4,t_5)=\left(\frac{i}{\hbar}\right)^5\langle[[[[[\tilde{p}_i(t),\tilde{p}_j(t_1)],\tilde{p}_k(t_2)],\tilde{p}_l(t_3)]\tilde{p}_m(t_4)],\tilde{p}_n(t_5)]\rangle \times H(t-t_1)H(t_1-t_2)H(t_2-t_3)H(t_3-t_4)H(t_4-t_5). \tag{9c}$$

Here $H(t)$ represents Heavysides step function. The perturbative procedure yields a full time ordering of the interactions: the interaction at t_2 always occurs before the interaction at t_1 and so on.

B. The Born–Oppenheimer approximation

In transparent media, where all optical frequencies are well below any electronic resonances, the electrons follow the applied field and the moving nuclei adiabatically. Then, the Born–Oppenheimer approximation (BOA) holds and can be incorporated in the perturbative calculation of the nonlinear polarization.[33] The electrons can be eliminated from the general treatment of Sec. II A, by assuming that they are always in their ground state, irrespective of the nuclear configuration and the external field strength. In the unperturbed system, their presence manifests itself as an effective potential for nuclear motion. The unperturbed Hamiltonian H_0^{BO} in the BOA is given by the sum of the kinetic energy of the nuclei T_N, the Coulomb interaction among them, and the ground state energy W_{00} of the electrons

$$H_0^{\mathrm{BO}}=T_N+\sum_{\alpha\neq\beta}\frac{e_\alpha e_\beta}{|\mathbf{r}_\alpha-\mathbf{r}_\beta|}+W_{00}. \tag{10}$$

Here the sum is to be taken over the nuclei only. Since the electrons follow the applied optical field instantaneously, the change of their ground state energy at any moment can be described by time-independent perturbation theory. This yields an expansion of the electron ground state energy W_0 in powers of the electric field:

$$W_0=W_{00}-(\mu_iE_i+\tfrac{1}{2}\alpha_{ij}E_iE_j+\tfrac{1}{3}\beta_{ijk}E_iE_jE_k+\tfrac{1}{4}\gamma_{ijkl}E_iE_jE_kE_l+\tfrac{1}{5}\epsilon_{ijklm}E_iE_jE_kE_lE_m+\tfrac{1}{6}\zeta_{ijklmn}E_iE_jE_kE_lE_mE_n+\cdots). \tag{11}$$

Every coefficient $W_{00},\mu_i,\alpha_{ij},\ldots$ in this expansion depends explicitly, but in a generally unknown way, on the nuclear coordinates. W_{00} is again the electronic ground state energy in absence of any electric field, while μ_i is the electronic dipole moment, α_{ij} is the electronic susceptibility, and $\beta_{ijk},\gamma_{ijkl},\ldots$ are higher-order hyperpolarizabilities.

Now, the interaction Hamiltonian $H_I^{\mathrm{BO}}(t)$ consists of an electronic part, that is due to the change of the electronic ground state energy by the applied field and given by the term in the brackets in Eq. (11), and a nuclear part due to direct coupling of the optical field with the charged nuclei[33]

$$H_I^{\mathrm{BO}}(t)=-(m_iE_i+\tfrac{1}{2}\alpha_{ij}E_iE_j+\tfrac{1}{3}\beta_{ijk}E_iE_jE_k+\tfrac{1}{4}\gamma_{ijkl}E_iE_jE_kE_l+\tfrac{1}{5}\epsilon_{ijklm}E_iE_jE_kE_lE_m+\tfrac{1}{6}\zeta_{ijklmn}E_iE_jE_kE_lE_mE_n+\cdots). \tag{12}$$

Here $\mathbf{m}\equiv\boldsymbol{\mu}+\Sigma e_\alpha\mathbf{r}_\alpha$ is the electric dipole in absence of the optical field; it depends only on the nuclear configuration.

The total dipole operator $\mathbf{p}^{\mathrm{BO}}$ also consists of a nuclear and an electronic part

$$\mathbf{p}^{\mathrm{BO}}=\left(\sum_\alpha e_\alpha\mathbf{r}_\alpha-\frac{dW_0}{d\mathbf{E}}\right)=-\frac{dH_I^{\mathrm{BO}}}{d\mathbf{E}}. \tag{13}$$

Using Eq. (12), it becomes clear that $\mathbf{p}^{\mathrm{BO}}$ is explicitly field dependent

$$p_i^{\mathrm{BO}}=m_i+\alpha_{ij}E_j+\beta_{ijk}E_jE_k+\gamma_{ijkl}E_jE_kE_l+\epsilon_{ijklm}E_jE_kE_lE_m+\zeta_{ijklmn}E_jE_kE_lE_mE_n+\cdots. \tag{14}$$

The prefactors 1/2, 1/3, 1/4, and so on in the expansion of W_0 [Eq. (11)] were chosen such that they disappear here. This is due to the fact that the polarizability tensors are totally symmetric (Kleinman symmetry).[78]

Using the reduced Hamiltonian H_0^{BO} of the unperturbed system [Eq. (10)], the interaction Hamiltonian H_I^{BO} [Eq. (12)], and the dipole operator $\mathbf{p}^{\mathrm{BO}}$ [Eq. (14)], the nonlinear

response functions can be calculated without explicit consideration of the electronic degrees of freedom. The polarization is now given by

$$P_i(t)=\langle (U^{\mathrm{BO}}(t))^{-1} p_i^{\mathrm{BO}} U^{\mathrm{BO}}(t)\rangle, \tag{15}$$

where the expectation value is calculated by tracing over the nuclear subspace only. The time evolution operator $U^{\mathrm{BO}}(t)$ in the BOA obeys an equation of motion similar to Eq. (5), but now H_0 and $H_I(t)$ have to be replaced by H_0^{BO} and $H_I^{\mathrm{BO}}(t)$, respectively. When $U^{\mathrm{BO}}(t)$ is again solved iteratively, the result for the dipole operator in the Heisenberg representation, up to the fifth iteration step, is

$$\begin{aligned}
&(U^{\mathrm{BO}}(t))^{-1} p_i^{\mathrm{BO}} U^{\mathrm{BO}}(t)\\
&=\tilde{p}_i^{\mathrm{BO}}(t)+\left(\frac{-i}{\hbar}\right)\int_{-\infty}^{t} dt_1[\tilde{p}_i^{\mathrm{BO}}(t),\tilde{H}_I^{\mathrm{BO}}(t_1)]+\left(\frac{-i}{\hbar}\right)^2\int_{-\infty}^{t} dt_1\int_{-\infty}^{t_1} dt_2[[\tilde{p}_i^{\mathrm{BO}}(t),\tilde{H}_I^{\mathrm{BO}}(t_1)],\tilde{H}_I^{\mathrm{BO}}(t_2)]\\
&+\left(\frac{-i}{\hbar}\right)^3\int_{-\infty}^{t} dt_1\int_{-\infty}^{t_1} dt_2\int_{-\infty}^{t_2} dt_3[[[\tilde{p}_i^{\mathrm{BO}}(t),\tilde{H}_I^{\mathrm{BO}}(t_1)],\tilde{H}_I^{\mathrm{BO}}(t_2)],\tilde{H}_I^{\mathrm{BO}}(t_3)]\\
&+\left(\frac{-i}{\hbar}\right)^4\int_{-\infty}^{t} dt_1\int_{-\infty}^{t_1} dt_2\int_{-\infty}^{t_2} dt_3\int_{-\infty}^{t_3} dt_4[[[[\tilde{p}_i^{\mathrm{BO}}(t),\tilde{H}_I^{\mathrm{BO}}(t_1)],\tilde{H}_I^{\mathrm{BO}}(t_2)],\tilde{H}_I^{\mathrm{BO}}(t_3)],\tilde{H}_I^{\mathrm{BO}}(t_4)]\\
&+\left(\frac{-i}{\hbar}\right)^5\int_{-\infty}^{t} dt_1\int_{-\infty}^{t_1} dt_2\int_{-\infty}^{t_2} dt_3\int_{-\infty}^{t_3} dt_4\int_{-\infty}^{t_4} dt_5[[[[[\tilde{p}_i^{\mathrm{BO}}(t),\tilde{H}_I^{\mathrm{BO}}(t_1)],\tilde{H}_I^{\mathrm{BO}}(t_2)],\tilde{H}_I^{\mathrm{BO}}(t_3)],\tilde{H}_I^{\mathrm{BO}}(t_4)],\tilde{H}_I^{\mathrm{BO}}(t_5)].
\end{aligned} \tag{16}$$

$\tilde{A}(t)$ now means that operator A is transformed to the interaction picture in the BOA. Its time evolution is governed by the time evolution operator $U_0^{\mathrm{BO}}(t)=\exp(-iH_0^{\mathrm{BO}}t/\hbar)$.

Analogous to Sec. II A, the response functions can be calculated by inserting Eqs. (12) and (14) for $H_I^{\mathrm{BO}}(t)$ and $p_i^{\mathrm{BO}}(t)$ in Eq. (16), and comparing the result to Eqs. (2). Since both operators are power series in the applied field, several terms of Eq. (16) contribute to a given order in **E**. For example, the result for linear response is:

$$R_{ij}^{(1)}(t,t_1)=\langle \alpha_{ij}\rangle \delta(t-t_1)+\frac{i}{\hbar}\langle[\tilde{m}_i(t),\tilde{m}_j(t_1)]\rangle H(t-t_1). \tag{17}$$

The first part results from the first term of Eq. (16), and is due to linear electronic polarization. It is instantaneous and gives rise to Rayleigh scattering, where the frequencies of the annihilated and created photons are equal. The second part originates from the second term of Eq. (16) and describes FIR absorption, which can be neglected when the frequency of the applied field is well above the nuclear resonances.

C. Third-order nonlinear optical response

In centrosymmetric media there are no second-order nonlinear optical effects, so we continue our treatment with the third-order response. The corresponding response function can be evaluated by collecting all terms in Eq. (16) that are of third order in **E**. The result is

$$R_{ijkl}^{(3)}(t,t_1,t_2,t_3)=\langle \gamma_{ijkl}\rangle \delta(t-t_1)\delta(t_1-t_2)\delta(t_2-t_3) \tag{18a}$$

$$+\frac{i}{\hbar}\langle[\tilde{\alpha}_{ij}(t),\tfrac{1}{2}\tilde{\alpha}_{kl}(t_2)]\rangle \delta(t-t_1)H(t_1-t_2)\delta(t_2-t_3) \tag{18b}$$

$$+\frac{i}{\hbar}\langle[\tilde{m}_i(t),\tfrac{1}{3}\tilde{\beta}_{jkl}(t_1)]\rangle H(t-t_1)\delta(t_1-t_2)\delta(t_2-t_3) \tag{18c}$$

$$+\frac{i}{\hbar}\langle[\tilde{\beta}_{ijk}(t),\tilde{m}_l(t_3)]\rangle \delta(t-t_1)\delta(t_1-t_2)H(t_2-t_3) \tag{18d}$$

$$+\left(\frac{i}{\hbar}\right)^2\langle[[\tilde{m}_i(t),\tilde{m}_j(t_1)],\tfrac{1}{2}\tilde{\alpha}_{kl}(t_2)]\rangle H(t-t_1)H(t_1-t_2)\delta(t_2-t_3) \tag{18e}$$

$$+\left(\frac{i}{\hbar}\right)^2\langle[[\tilde{m}_i(t),\tfrac{1}{2}\tilde{\alpha}_{jk}(t_1)],\tilde{m}_l(t_3)]\rangle H(t-t_1)\,\delta(t_1-t_2)H(t_2-t_3) \tag{18f}$$

$$+\left(\frac{i}{\hbar}\right)^2\langle[[\tilde{\alpha}_{ij}(t),\tilde{m}_k(t_2)],\tilde{m}_l(t_3)]\rangle\,\delta(t-t_1)H(t_1-t_2)H(t_2-t_3) \tag{18g}$$

$$+\left(\frac{i}{\hbar}\right)^3\langle[[[\tilde{m}_i(t),\tilde{m}_j(t_1)],\tilde{m}_k(t_2)],\tilde{m}_l(t_3)]\rangle H(t-t_1)H(t_1-t_2)H(t_2-t_3). \tag{18h}$$

Here the first four terms of Eq. (16) yield parts (18a), (18b)–(18d), (18e)–(18g), and (18h), respectively. They describe distinct physical processes. In Eq. (18a) the optical interaction occurs through the instantaneous nonlinear electronic hyperpolarizability, where three photons excite virtual levels to generate a fourth one. This process is depicted in an energy level diagram in Fig. 2(a). Part (18b) describes Rayleigh/Raman scattering. This is shown schematically in Fig. 2(b): at time $t_2=t_3$ a coherent superposition of nuclear states is created, that after a propagation period $\tau_1\equiv t_1-t_2$ is converted into an optical signal at time $t=t_1$. Although an energy level representation can give a raw impression of these processes, the dynamics are better characterized by looking at the quantum evolution of the nuclear states in Liouville space. This can be depicted in the form of double-sided Feynman diagrams. For the electronic hyperpolarizability [Eq. (18a)], this is shown in Fig. 3(a), while the Raman process [Eq. 18(b)] is described by the sum of two diagrams, shown as Figs. 3(b.1) and 3(b.2).

All remaining terms contain the dipole moment operator and vanish when all applied frequencies are well above the nuclear resonances. Parts (18c)–(18g) may be observed in double-resonance experiments, that have not been reported yet. The last part (18h) describes resonant IR four-wave mixing experiments like pump–probe, photon–echo, and grating scattering, that all have been performed on various samples.[57–61] A detailed description is analogous to that of resonant four-wave mixing experiments with visible light, and is presented in standard textbooks on nonlinear spectroscopy.[79,80] Hence, when the applied frequencies are well above all nuclear resonances, the third-order response function consists of only two terms [Eqs. (18a) and (18b)]. These will be employed in Sec. III to derive expressions for the femtosecond optical Kerr effect and grating scattering experiments.

D. Fifth-order nonlinear optical response

The fifth-order response function is obtained by inserting the expansions of the interaction Hamiltonian [Eq. (12)] and the dipole operator [Eq. (14)] in Eq. (16), taking the expectation value [Eq. (15)], collecting all terms that are of fifth order in the electric field, and comparing the result to Eq. (2c). In this way, we find that the first and sixth term of Eq. (16) each yield one contribution, the second and the fifth term both give five, and the third and fourth term each yield ten. Thus, the full response function consists of 32 independent terms. The complete expression is given in Appendix A.

In the remainder of this paper we will concentrate on the situation where all applied optical fields are far above the nuclear resonances. In this case all terms containing the electric dipole moment operator m are negligible. Term (A4) of the complete expression describes hyper Rayleigh–Raman scattering, where two of the involved photons are at the second-harmonic frequency of the applied radiation.[81,82] When only the fundamental wavelength is detected, this term can be ignored. Then, the fifth-order response function consists only of terms (A1), (A3), (A5), and (A12)

$$R^{(5)}_{ijklmn}=\langle\zeta_{ijklmn}\rangle\,\delta(t-t_1)\,\delta(t_1-t_2)\,\delta(t_2-t_3)\,\delta(t_3-t_4)\,\delta(t_4-t_5) \tag{19a}$$

$$+\frac{i}{\hbar}\langle[\tilde{\alpha}_{ij}(t),\tfrac{1}{4}\tilde{\gamma}_{klmn}(t_2)]\rangle\,\delta(t-t_1)H(t_1-t_2)\,\delta(t_2-t_3)\,\delta(t_3-t_4)\,\delta(t_4-t_5) \tag{19b}$$

$$+\frac{i}{\hbar}\langle[\tilde{\gamma}_{ijkl}(t),\tfrac{1}{2}\tilde{\alpha}_{mn}(t_4)]\rangle\,\delta(t-t_1)\,\delta(t_1-t_2)\,\delta(t_2-t_3)H(t_3-t_4)\,\delta(t_4-t_5) \tag{19c}$$

$$+\left(\frac{i}{\hbar}\right)^2\langle[[\tilde{\alpha}_{ij}(t),\tfrac{1}{2}\tilde{\alpha}_{kl}(t_2)],\tfrac{1}{2}\tilde{\alpha}_{mn}(t_4)]\rangle\,\delta(t-t_1)H(t_1-t_2)\,\delta(t_2-t_3)H(t_3-t_4)\,\delta(t_4-t_5). \tag{19d}$$

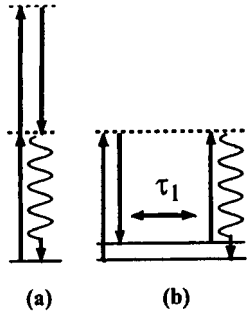

FIG. 2. Energy level diagrams for third-order scattering due to (a) electronic hyperpolarizability, and (b) Rayleigh/Raman scattering. These processes are described by Eqs. (18a) and (18b), respectively. The dashed horizontal lines are virtual levels that have an infinitely short lifetime in the BOA. The solid horizontal lines depict real nuclear states in the electronic ground state. Solid arrows indicate applied photons, while the wavy line symbolizes the generated photon.

The processes that correspond to these four terms are depicted in an energy level scheme in Fig. 4. The first term is due to the instantaneous electronic hyperpolarizability, where five photons, via virtual electronic levels, generate a sixth one [Fig. 4(a)]. It contains no information on the nuclear dynamics. The second term describes excitation of a nuclear coherence by a four-photon process, governed by the coordinate dependent hyperpolarizability $\gamma(q)$. After a propagation period $\tau_2=t_1-t_2$ the nuclear coherence is converted into an optical signal by a Raman process, governed by the coordinate dependent polarizability $\alpha(q)$, as shown in Fig. 4(b). Such a sequence of interactions was shown to be responsible for subharmonic Raman resonances in fifth-order frequency-domain spectroscopy in gases.[83] The third term is the mirror image of the second one: the nuclear coherence is excited by Raman scattering and after a propagation period $\tau_1=t_3-t_4$ it is converted into an optical signal by a four-photon process [Fig. 4(c)]. Since the second and third term each depend on only one propagation time, they contain information on the nuclear dynamics, similar to the usual third-order Raman term, discussed in Sec. II C.

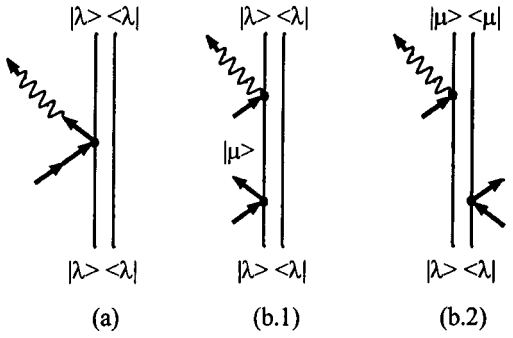

FIG. 3. Feynman diagrams for the third-order scattering of Fig. 2. The nuclear dynamics during excitation of virtual states is neglected in the BOA. The coupling is governed by the polarizability α when two photons meet at a vertex, and by the hyperpolarizability γ when four photons are involved. Multiple arrows at a vertex means that all possible field permutations should be taken. The wavy line is the generated photon. One diagram (a) describes instantaneous scattering due to electronic hyperpolarizability [see Fig. 2(a)], while two diagrams [(b.1) and (b.2)] are required to describe Raman scattering [see Fig. 2(b)].

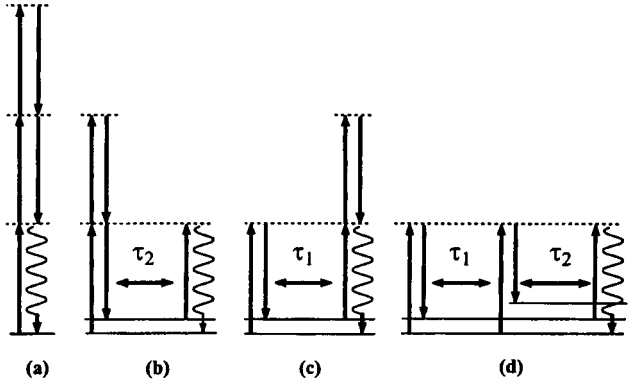

FIG. 4. Energy level diagrams for fifth-order scattering. These processes are described by Eqs. (19a)–(19d). Interactions and energy levels are defined as in Fig. 2. (a) Pure electronic fifth-order polarization gives rise to instantaneous scattering. (b) Hyper-Raman scattering excites a nuclear coherence, that after a propagation time τ_2 is converted into an optical signal by an ordinary Raman process. (c) Raman scattering is followed after time τ_1 by a four-photon hyper-Raman interaction. (d) Three subsequent scattering events give rise to a two-dimensional Raman process, that contains both propagation times τ_1 and τ_2.

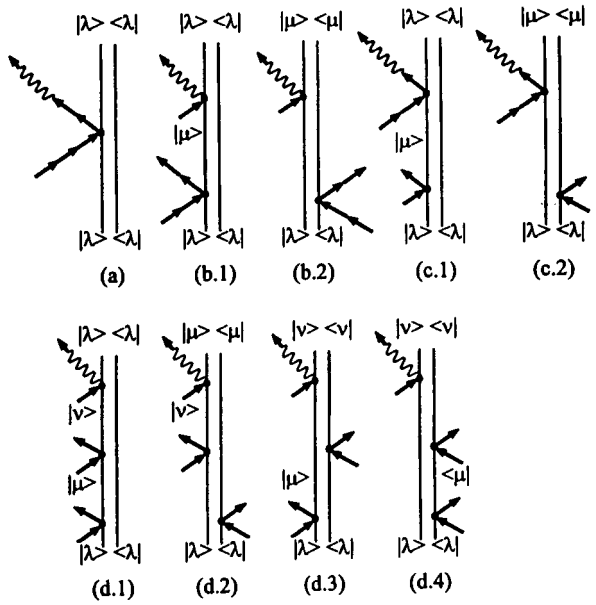

FIG. 5. Feynman diagrams for fifth-order scattering: (a)–(d) refer to the corresponding processes of Fig. 4. The definition of vertices and arrows is as in Fig. 3. (a) Scattering due to the purely electronic hyperpolarizability ζ is depicted by one diagram. (b) and (c) Both processes involving hyper-Raman scattering consist of the sum of two diagrams. (d) The description of two-dimensional Raman scattering requires four diagrams. In the inhomogeneous limit of nuclear dynamics, these diagrams contain the possibility of rephasing of nuclear coherence, which may yield a motional echo.

The term (19d) describes three subsequent Raman scattering processes [Fig. 4(d)]. It contains two independent propagation periods $\tau_1=t_3-t_4$ and $\tau_2=t_1-t_2$, and therefore has the capability to provide additional dynamical information, not available from lower-order experiments. It is this term that was first discussed in the work of Tanimura and Mukamel,[65] which was followed by a number of other theoretical[68,69] and experimental papers.[70–72,74,75] This process allows one, in principle, to distinguish between homogeneous and inhomogeneous contributions to line broadening of nuclear transitions. Thereby, it provides information on the time scale of structural fluctuations in liquids, as will be discussed in Sec. III. The Liouville-space double-sided Feynman diagrams of all fifth-order terms of Eq. (19) are depicted in Fig. 5. The first term can be described by a single diagram [Fig. 5(a)], the second and third terms by sums of two diagrams [Figs. 5(b.1) and 5(b.2), and Figs. 5(c.1) and 5(c.2), respectively], and the last term with two propagation times needs four diagrams to capture all possible pathways of nuclear propagation [Figs. 5(d.1)–5(d.4)].[84]

The relative magnitude of the four terms of Eq. (19) depends in general on the investigated sample and the wavelength of the radiation. When the energy of two or three photons becomes (pre) resonant with electronic levels, the processes that depend on the corresponding hyperpolarizabilities can be resonantly enhanced. The contribution due to the purely electronic polarization can be easily distinguished experimentally, since it is instantaneous. The distinction between the second and third processes and the fourth one, however, is less straightforward. For a reliable interpretation of the experimental results, it is essential to assign the signal unambiguously to one of the processes of Eq. (19), since they contain entirely different dynamical information.[76]

The theoretical approach, sketched in this section, is easily extended to higher order processes. For instance, the seventh-order response, using nonresonant optical fields and excluding second-harmonic detection, contains eight different terms. Of these, one is instantaneous, three contain a single propagation period, three others contain two propagation periods, and in one process three independent propagation times occur. The Raman echo is one of the effects described by this last term. Again, new information on the nuclear dynamics can be expected. Here, we will not discuss the seventh-order response any further, since the highest-order nonlinear experiments on low frequency modes in liquids, reported so far, are of fifth order.[70–75]

III. OPTICAL DYNAMICS OF NUCLEAR MOTIONS IN LIQUIDS

The nonlinear optical theory of Sec. II can be employed to analyze third- and fifth-order experiments when a model for the nuclear motion is adopted. In Sec. III A, the response functions are first formulated in terms of nuclear eigenstates. These results are valid for any Hamiltonian and any functional form of the coordinate dependent (hyper) polarizability operators. Then, the assumption of harmonic nuclear motion is made, and the polarizability operators are expanded into a power series of the nuclear coordinate. In Sec. III B damping is treated in the weak coupling limit for level-dependent and level-independent decay rates. The results are compared to existing theory of Mukamel and co-workers.[65,68,69] Inhomogeneity of the nuclear spectrum leads to the generation of motional echoes in the fifth-order response. Model calculations are shown for the parameters of an intermolecular mode of liquid CS_2. In Sec. III C the nonlinear response is considered when two or more nuclear modes determine the optical response.

A. The nonlinear response of harmonic nuclear motion

For nonresonant radiation fields, the third-order polarization can be obtained by inserting Eqs. (18a) and (18b) in Eq. (2b), as discussed in Sec. II C, while the corresponding fifth-order polarization is found by inserting Eq. (19) in Eq. (2c), as discussed in Sec. II D. For simplicity, the tensorial notation of the response function will be suppressed from now on. It can be incorporated without major difficulties, to evaluate the polarization selectivity of the various contributions to the signals.[85,86] The response functions will be expressed in terms of the positive propagation times τ_1 and τ_2, instead of the absolute times $t_1,t_2,...$ (see Fig. 1). This is more convenient, since some of the absolute times were found to be identical under all circumstances (Sec. II). Thus, the third-order polarization can be written as

$$P^{(3)}(t)=E(t)\int_0^\infty d\tau_1 R^{(3)}(\tau_1)E^2(t-\tau_1), \tag{20}$$

where

$$R^{(3)}(\tau_1)=\langle\gamma\rangle\delta(\tau_1)+\frac{i}{2\hbar}\langle[\tilde{\alpha}(\tau_1),\tilde{\alpha}(0)]\rangle. \tag{21}$$

The two terms correspond to Figs. 2(a) and 2(b) and 3(a) and 3(b), respectively. The corresponding fifth-order polarization is

$$P^{(5)}(t)=E(t)\int_0^\infty d\tau_1\int_0^\infty d\tau_2\ R^{(5)}(\tau_1,\tau_2)E^2(t-\tau_1)\times E^2(t-\tau_1-\tau_2), \tag{22}$$

where

$$\begin{aligned}R^{(5)}(\tau_1,\tau_2)=&\langle\zeta\rangle\delta(\tau_1)\delta(\tau_2)\\&+\frac{i}{4\hbar}\langle[\tilde{\alpha}(\tau_2),\tilde{\gamma}(0)]\rangle\delta(\tau_1)\\&+\frac{i}{2\hbar}\langle[\tilde{\gamma}(\tau_1),\tilde{\alpha}(0)]\rangle\delta(\tau_2)\\&-\frac{1}{4\hbar^2}\langle[[\tilde{\alpha}(\tau_2+\tau_1),\tilde{\alpha}(\tau_1)],\tilde{\alpha}(0)]\rangle.\end{aligned} \tag{23}$$

These four terms correspond to Figs. 4(a)–4(d) and 5(a)–5(d), respectively. The meaning of these expressions be-

comes clear when the commutators are written out in their various factors, and the (hyper) polarizability operators are transformed back from the interaction picture

$$\langle\lambda|\tilde{A}(t)|\mu\rangle=\langle\lambda|A|\mu\rangle e^{i(\epsilon_\lambda-\epsilon_\mu)t/\hbar}\equiv A_{\lambda\mu}e^{i\omega_{\lambda\mu}t}. \tag{24}$$

Here, $|\lambda\rangle$,$|\mu\rangle$,... are the eigenstates of nuclear motion in the BOA, and the difference of energy eigenvalues is represented by $\epsilon_\lambda-\epsilon_\mu\equiv\hbar\omega_{\lambda\mu}$. The third- and fifth-order response functions in this representation read

$$R^{(3)}(\tau_1)=\langle\gamma\rangle\delta(\tau_1)-\frac{1}{\hbar}\sum_{\lambda,\mu}P(\lambda)\alpha_{\lambda\mu}(q)\alpha_{\mu\lambda}(q)\sin(\omega_{\lambda\mu}\tau_1), \tag{25}$$

$$\begin{aligned}R^{(5)}(\tau_1,\tau_2)=&\langle\zeta\rangle\delta(\tau_1)\delta(\tau_2)-\frac{1}{\hbar}\sum_{\lambda,\mu}P(\lambda)\alpha_{\lambda\mu}(q)\gamma_{\mu\lambda}(q)\\&\times[\tfrac{1}{2}\,\delta(\tau_1)\sin(\omega_{\lambda\mu}\tau_2)+\delta(\tau_2)\sin(\omega_{\lambda\mu}\tau_1)]\\&-\frac{1}{2\hbar^2}\sum_{\lambda,\mu,\nu}P(\lambda)\alpha_{\lambda\mu}(q)\alpha_{\mu\nu}(q)\alpha_{\nu\lambda}(q)\\&\times[\cos(\omega_{\lambda\mu}\tau_1+\omega_{\lambda\nu}\tau_2)\\&-\cos(\omega_{\lambda\mu}\tau_1+\omega_{\nu\mu}\tau_2)].\end{aligned} \tag{26}$$

In Eqs. (25) and (26), $P(\lambda)$ denotes the equilibrium distribution of states $|\lambda\rangle$. We want to stress that the treatment at this point does not depend on the specific forms of the Hamiltonian H_0^{BO} or the (hyper) polarizability operators $\alpha(q)$ and $\gamma(q)$. These general expressions, that we believe have not been published before, describe the third- and fifth-order nonlinear response due to nuclear motion under nonresonant excitation. The Feynman diagrams of Figs. 3 and 5 are pictorial representations of the involved quantum mechanical pathways. To calculate the matrix elements $\alpha_{\lambda\mu}$ and $\gamma_{\lambda\mu}$ a model has to be adopted for the nuclear motion and these polarizability operators.

For harmonic motion, the eigenstates $|\lambda\rangle$ are known, and the Hamiltonian and the harmonic coordinate can be expressed in terms of the raising and lowering operators $a^\dagger$ and a: $H_0^{\mathrm{BO}}=\hbar\omega(a^\dagger a+1/2)$ and $q=(\hbar/2m\omega)^{1/2}(a^\dagger+a)$. The coordinate dependence of the (hyper) polarizability operators α and γ is in general not known exactly, and usually expanded into a power series of q. When they do not depend on q at all, the (hyper-) Raman transition probabilities vanish. When α is linear in q and the hyperpolarizability γ can be neglected, the fifth-order response does not exist because two-quantum transitions are forbidden, and hence all diagrams of Fig. 5(d) vanish separately (see below). For seventh-order response, each diagram yields a finite contribution, but for level-independent damping the total response still does not exist. The reason is that the contributions from the various diagrams interfere destructively. When the decay rates are level dependent, this interference is not perfect, and hence the seventh-order response no longer vanishes.[87]

Thus, fifth-order experiments in harmonic systems are only possible when either α is nonlinear in q and/or the hyperpolarizability γ yields extra contributions. Here, we expand α up to second order in q: $\alpha(q)=\alpha_1 q+\alpha_2 q^2$, and γ, which is supposed to be smaller than α, up to first order, $\gamma(q)=\gamma_1 q$. Using these expansions, and writing q in terms of the raising and lowering operators $a^\dagger$ and a, the matrix elements $\alpha_{\lambda\mu}(q)$ and $\gamma_{\lambda\mu}(q)$ of Eqs. (25) and (26) are expressed in terms of the well-known harmonic oscillator matrix elements

$$\begin{aligned}&\langle\lambda|a^\dagger|\mu\rangle=\langle\mu|a|\lambda\rangle=\sqrt{\mu+1}\,\delta_{(\mu+1),\lambda},\\&\langle\lambda|a^\dagger a^\dagger|\mu\rangle=\langle\mu|aa|\lambda\rangle=\sqrt{(\mu+1)(\mu+2)}\,\delta_{(\mu+2),\lambda},\\&\langle\lambda|aa^\dagger|\mu\rangle=\langle\mu|aa^\dagger|\lambda\rangle=(\mu+1)\,\delta_{\mu,\lambda}.\end{aligned} \tag{27}$$

In this way, Eqs. (25) and (26) are easily evaluated. The general results, explicitly written in terms of the quantum states of the system, are shown in Appendix B. As discussed in Sec. III B, damping is included in the weak coupling limit. Here, we first treat the situation when damping is negligible, to show the general structure of the response functions. The third-order result then is

$$R^{(3)}(\tau_1)=\langle\gamma\rangle\delta(\tau_1)+\frac{\alpha_1^2}{2m\omega}\sin(\omega\tau_1)+\frac{\alpha_2^2\hbar}{2m^2\omega^2}\sum_{\lambda}(2\lambda+1)P(\lambda)\sin(2\omega\tau_1). \tag{28}$$

A one-quantum nuclear transition has a probability proportional to α_1, leading to oscillations at frequency ω. The second coefficient α_2 allows for two-quantum transitions, since q^2 contains a^2 and $(a^\dagger)^2$. This yields temperature dependent oscillations at 2ω. The corresponding fifth-order response function reads

$$\begin{aligned}R^{(5)}(\tau_1,\tau_2)=&\langle\zeta\rangle\delta(\tau_1)\delta(\tau_2)+\frac{\alpha_1\gamma_1}{4m\omega}\,\delta(\tau_1)\sin(\omega\tau_2)\\&+\frac{\alpha_1\gamma_1}{2m\omega}\,\delta(\tau_2)\sin(\omega\tau_1)\\&+\frac{\alpha_2^3\hbar}{2m^3\omega^3}\sum_{\lambda}(2\lambda+1)P(\lambda)\\&\times[\cos 2\omega\tau_1-\cos 2\omega(\tau_2+\tau_1)]\\&+\frac{\alpha_1^2\alpha_2}{4m^2\omega^2}[\cos\omega(\tau_1-\tau_2)-\cos\omega(\tau_1+\tau_2)\\&+\cos\omega\tau_1-\cos\omega(\tau_1+2\tau_2)].\end{aligned} \tag{29}$$

Note that the term proportional to $\cos\omega(2\tau_1+\tau_2)$ in the expression for $R^{(5)}(\tau_1,\tau_2)$ in Appendix B has disappeared here, due to perfect destructive interference of the involved quantum mechanical pathways. As will be discussed in Sec. III B, the interference is destroyed when the damping of the motion

is explicitly level dependent. Then, the fifth-order optical response will indeed contain a part that oscillates with $\cos\,\omega(2\tau_1+\tau_2)$.

The first term of Eq. (29) is due to the hyperpolarizability ζ [Figs. 4(a) and 5(a)], and contains no information on the nuclear dynamics. The second [Figs. 4(b) and 5(b)] and third terms [Figs. 4(c) and 5(c)] are similar to the third-order response Eq. (28). They contain the same dynamical information but one of the two temporally separated interactions is an instantaneous four photon interaction governed by the hyperpolarizability γ. The last two terms describe the temporally two-dimensional Raman process of Figs. 4(d) and 5(d). The first of these, consisting of two parts, involves three transitions that all depend on q^2. The part proportional to $\cos[2\omega(\tau_1+\tau_2)]$ is generated by a two-quantum transition, followed by a zero-quantum transition and another two-quantum transition after propagations τ_1 and τ_2, respectively. The zero-quantum transition, which does not change the state of the system, is possible because q^2 comprises a term proportional to $(2a^{\dagger}a+1)$. The system is in a coherent two-quantum superposition state, $|\lambda\rangle\langle\lambda\pm2|$ or $|\lambda\pm2\rangle\langle\lambda|$, during both propagation periods. The part proportional to $\cos[2\omega\tau_1]$ is caused by two subsequent two-quantum transitions, followed by a zero-quantum transition. During τ_1 the system is in a coherent two-quantum superposition state, while during τ_2 it is in a population state, $|\lambda\rangle\langle\lambda|$ or $|\lambda\pm2\rangle\langle\lambda\pm2|$.

The last term of Eq. (29), which consists of four parts, always comprises two one-quantum transitions and one two-quantum transition, in different time order. The states of the system during the two propagation periods can be easily constructed from the corresponding Feynman diagrams [Fig. 5(d)] or the expression for $R^{(5)}(\tau_1,\tau_2)$ in Appendix B, in which the states are explicitly shown. This term is proportional to the inverse of the oscillation frequency squared, while the pure two-quantum one is inversely proportional to ω^3. Note that these are stronger frequency dependencies than that of the leading term of the third-order nuclear response $(\sim\omega^{-1})$.

B. Relaxation phenomena

So far, the treatment of the nonlinear optical response is incomplete, in the sense that damping of the induced nuclear motion is not included, yet. In condensed matter it is generally impossible to describe all degrees of freedom exactly. Usually, a few degrees of freedom that dominate the optical response are described explicitly and called ''the system.'' In our case this is the harmonic oscillation of Sec. III A. All other variables are accounted for by an implicit description of their influence on the dynamics of the system. They form the ''heat bath,'' which is responsible for dephasing and relaxation phenomena of the system. The separation of system and bath variables is not unique and depends on the desired level of sophistication.[79,88]

The effect of the bath can be easily incorporated phenomenologically, when the coupling between the system and the heat-bath is weak and fluctuates very fast (Markovian dynamics). Then, exponential decay rates can be introduced to describe the damping of the density matrix elements $|\lambda\rangle\langle\mu|$. This is analogous to adding an imaginary part to the system transition frequencies, according to: $\omega_{\lambda\mu}\rightarrow\omega_{\lambda\mu}+i\Gamma_{\lambda\mu}$, where $\Gamma_{\lambda\mu}=\Gamma_{\mu\lambda}=(\gamma_\lambda+\gamma_\mu)/2+\Gamma^*_{\lambda\mu}$. Here $\Gamma^*_{\lambda\mu}$ is the pure dephasing rate and $1/\gamma_\lambda$ is the lifetime of state λ. Note that the real part of the frequency remains unchanged. When the decay is assumed to be independent of the quantum numbers of the involved states, the damping is fully characterized by a single population decay rate γ and the dephasing rates Γ_1 and Γ_2, which describe the decay of the one- and two-quantum coherences $|\lambda\pm1\rangle\langle\lambda|$ and $|\lambda\pm2\rangle\langle\lambda|$, respectively. The third- and fifth-order responses are then easily calculated from the general expressions in Appendix B. The results are

$$R^{(3)}(\tau_1)=\langle\gamma\rangle\,\delta(\tau_1)+\frac{\alpha_1^2}{2m\omega}\,e^{-\Gamma_1\tau_1}\,\sin(\omega\tau_1)+\frac{\alpha_2^2\hbar}{2m^2\omega^2}\sum_{\lambda}\,(2\lambda+1)P(\lambda)e^{-\Gamma_2\tau_1}\,\sin(2\omega\tau_1), \tag{30}$$

$$\begin{aligned}R^{(5)}(\tau_1,\tau_2)=&\langle\zeta\rangle\,\delta(\tau_1)\,\delta(\tau_2)+\frac{\alpha_1\gamma_1}{4m\omega}\,\delta(\tau_1)e^{-\Gamma_1\tau_2}\,\sin(\omega\tau_2)+\frac{\alpha_1\gamma_1}{2m\omega}\,\delta(\tau_2)e^{-\Gamma_1\tau_1}\,\sin(\omega\tau_1)\\&+\frac{\alpha_2^3\hbar}{2m^3\omega^3}\sum_{\lambda}\,(2\lambda+1)P(\lambda)e^{-\Gamma_2\tau_1}[e^{-\gamma\tau_2}\,\cos\,2\omega\tau_1-e^{-\Gamma_2\tau_2}\,\cos\,2\omega(\tau_2+\tau_1)]\\&+\frac{\alpha_1^2\alpha_2}{4m^2\omega^2}\,e^{-\Gamma_1\tau_1}[e^{-\Gamma_1\tau_2}\,\cos\,\omega(\tau_1-\tau_2)-e^{-\Gamma_1\tau_2}\,\cos\,\omega(\tau_1+\tau_2)+e^{-\gamma\tau_2}\,\cos\,\omega\tau_1-e^{-\Gamma_2\tau_2}\,\cos\,\omega(\tau_1+2\tau_2)].\end{aligned} \tag{31}$$

There are more sophisticated ways to account for dissipation in quantum systems that do not rely on the weak coupling or Markovian limits.[66] Grabert *et al.*[89] treated dephasing and relaxation in a fully quantum mechanical context, by linear coupling of the system with a bath, consisting of an ensemble of quantum oscillators. It is then possible to eliminate the bath coordinates and to derive reduced expressions for the system dynamics. This theory was applied to nonlinear optical experiments by Tanimura and Mukamel.[65,67] Here, we do not repeat the details of this theory but only quote the main result. The third- and fifth-order response was calculated in lowest order of q. In the limit of the frequency-independent damping rate γ, and provided that there is no inhomogeneous distribution of oscillator eigenfrequencies, their expressions for the response functions can be rewritten to resemble parts of our Eqs. (30) and (31)

$$R^{(3)}(\tau_1)\sim\exp\left(-\frac{\gamma\tau_1}{2}\right)\sin\,\Omega\tau_1, \tag{32}$$

$$\begin{aligned}R^{(5)}(\tau_1,\tau_2)\sim&\exp\left(-\frac{\gamma(\tau_1+\tau_2)}{2}\right)[\cos\,\Omega(\tau_1-\tau_2)\\&-\cos\,\Omega(\tau_1+\tau_2)]\\&+\exp\left(-\frac{\gamma(\tau_1+2\tau_2)}{2}\right)\\&\times[\cos\,\Omega\tau_1-\cos\,\Omega(\tau_1+2\tau_2)].\end{aligned} \tag{33}$$

Here, $\Omega=(\omega^2-\gamma^2/4)^{1/2}$ is the reduced eigenfrequency of the underdamped oscillator when $\omega>\gamma/2$ holds. For an overdamped oscillator ($\omega<\gamma/2$), Eqs. (32) and (33) have to be continued analytically: the reduced eigenfrequency is then $\Omega=(\gamma^2/4-\omega^2)^{1/2}$, and the sin and cos have to be replaced by sinh and cosh. In contrast to the phenomenological weak coupling model, the Brownian oscillator treatment accounts for the frequency shift of a damped oscillator and for a continuous change from underdamped to overdamped motion, when the damping rate γ is increased.

Equations (30) and (31) can also be compared to expressions derived by Leegwater and Mukamel for the nonlinear optical response in the limit of classical nuclear motion.[68] Unfortunately, a number of mathematical errors were made in that paper, as was later realized by Khidekel and Mukamel.[69] Those authors derived expressions very similar to ours, except for a few sign errors in the various terms. Also, rather unrealistic decay functions were calculated, since Lorentzian inhomogeneity was taken as the only damping mechanism. As a consequence the fifth-order response contains terms that do not decay at all, due to perfect rephasing of macroscopic coherence.[69]

Equations (32) and (33) can be directly compared to Eqs. (30) and (31), when $\Gamma_1=\frac{1}{2}\Gamma_2=\frac{1}{2}\gamma$ is assumed to hold. Then, apart from the renormalization of the oscillator frequency, Eq. (32) is identical to the lowest order term ($\sim q$) of Eq. (30), and Eq. (33) is identical to the lowest order term ($\sim q^3$) of the two-dimensional part of Eq. (31). The equality of the damping parameters suggest that the dephasing rate in Refs. 65 and 67 is lifetime limited ($\Gamma_1=\frac{1}{2}\gamma$), and increases linearly with the number of quanta involved in the transition ($\Gamma_1=\frac{1}{2}\Gamma_2$). The combination of these two requirements, however, is incompatible with the assumption of state independent damping parameters that was made by us here and also by Tanimura and Mukamel.[65,67] In fact, it can be shown[90–93] that a harmonic system, linearly coupled to a bath, has a lifetime that is inversely proportional to the quantum number of the state, while quadratic coupling gives rise to a pure dephasing rate that is proportional to the square of the difference between the quantum numbers of two states

$$\Gamma_{\lambda\mu}=\tfrac{1}{2}[(\lambda+\mu)(1+\eta)+2\eta]\gamma+(\lambda-\mu)^2\Gamma^*. \tag{34}$$

Here $\eta=\exp(-\hbar\omega/kT)$ is the Boltzmann factor that results from detailed balancing of the upward and downward transition probabilities, as is briefly explained in Appendix B. Note that the damping rates $\Gamma_{\lambda\mu}$ have now acquired an explicit temperature and frequency dependence. When such quantum number dependence is introduced, the third-order response function of Appendix B can be written as

$$\begin{aligned}R^{(3)}(\tau_1)=&\langle\gamma\rangle\,\delta(\tau_1)+\frac{\alpha_1^2}{2m\omega}\frac{(1-\eta)^2}{(1-\eta e^{-\gamma\tau_1(1+\eta)})^2}\\&\times\exp-\{[\Gamma^*+\tfrac{1}{2}\gamma(1+3\eta)]\tau_1\}\sin\,\omega\tau_1\\&+\frac{2\alpha_2^2\hbar}{(2m\omega)^2}\frac{(1-\eta)^2(1+\eta)}{(1-\eta e^{-\gamma\tau_1(1+\eta)})^3}\\&\times\exp\{-[4\Gamma^*+\gamma(1+2\eta)]\tau_1\}\sin\,2\omega\tau_1.\end{aligned} \tag{35}$$

In the limit of low temperature ($T\to 0$), this reduces to Eq. (30) with $\Gamma_1=\Gamma^*+\frac{1}{2}\gamma$ and $\Gamma_2=4\Gamma^*+\gamma$. This is consistent with the definition of the damping according to Eq. (34), since for $T\to 0$ the sin $\omega\tau_1$ term is solely due to the superpositions $|0\rangle\langle 1|$ and $|1\rangle\langle 0|$, while the sin $2\omega\tau_1$ term results from the superpositions $|0\rangle\langle 2|$ and $|2\rangle\langle 0|$. As the temperature is raised, the decay rates become faster [Eq. (34)] and states with shorter lifetimes become populated. This leads to increased damping of the third-order response function.

The corresponding fifth-order response function reads

$$R^{(5)}(\tau_1,\tau_2)=\langle\zeta\rangle\delta(\tau_1)\delta(\tau_2)+\frac{\alpha_1\gamma_1}{2m\omega}(1-\eta)^2\Bigg(\frac{\exp\{-[\Gamma^*+\frac{1}{2}\gamma(1+3\eta)]\tau_2\}}{(1-\eta\exp[-\gamma(1+\eta)\tau_2])^2}\frac{1}{2}\delta(\tau_1)\sin\omega\tau_2+\frac{\exp\{-[\Gamma^*+\frac{1}{2}\gamma(1+3\eta)]\tau_1\}}{(1-\eta\exp[-\gamma(1+\eta)\tau_1])^2}\delta(\tau_2)\sin\omega\tau_1\Bigg)$$

$$+\frac{\alpha_2^3\hbar}{2(2m\omega)^3}(1-\eta)^2(1+\eta)\Bigg(-\frac{8\exp\{-[4\Gamma^*+\gamma(1+2\eta)](\tau_1+\tau_2)\}}{(1-\eta\exp\{-\gamma(1+\eta)(\tau_1+\tau_2)\})^3}\cos 2\omega(\tau_1+\tau_2)$$

$$+\frac{2\{5\exp[-2\gamma(1+\eta)\tau_2]-1+(\exp[-2\gamma(1+\eta)\tau_2]-5)\eta\exp[-\gamma(1+\eta)(\tau_1+\tau_2)]\}\exp\{-[4\Gamma^*+\gamma(1+2\eta)]\tau_1-\gamma\eta\tau_2\}}{(1-\eta\exp[-\gamma(1+\eta)(\tau_1+\tau_2)])^4}\cos 2\omega\tau_1\Bigg)$$

$$+\frac{\alpha_1^2\alpha_2}{2(2m\omega)^2}(1-\eta)^2\Bigg(\frac{2(\exp[-\gamma(1+\eta)\tau_2]-\eta\exp[-\gamma(1+\eta)\tau_1])\exp\{-[\Gamma^*+\frac{1}{2}\gamma(1+3\eta)](\tau_1+\tau_2)\}}{(1-\eta\exp[-\gamma(1+\eta)(\tau_1+\tau_2)])^3}\cos\omega(\tau_1-\tau_2)$$

$$-\frac{2\exp\{-[\Gamma^*+\frac{1}{2}\gamma(1+3\eta)](\tau_1+\tau_2)\}}{(1-\eta\exp[-\gamma(1+\eta)(\tau_1+\tau_2)])^2}\cos\omega(\tau_1+\tau_2)$$

$$+\frac{\{3\exp[-\gamma(1+\eta)\tau_2]-1+(\exp[-\gamma(1+\eta)\tau_2]-3)\eta\exp[-\gamma(1+\eta)(\tau_1+\tau_2)]\}\exp\{-[\Gamma^*+\frac{1}{2}\gamma(1+3\eta)]\tau_1-\gamma\eta\tau_2\}}{(1-\eta\exp[-\gamma(1+\eta)(\tau_1+\tau_2)])^3}\cos\omega\tau_1$$

$$-\frac{2(1-\eta\exp[-\gamma(1+\eta)\tau_1])\exp\{-[\Gamma^*+\frac{1}{2}\gamma(1+3\eta)]\tau_1-[4\Gamma^*+\gamma(1+2\eta)]\tau_2\}}{(1-\eta\exp[-\gamma(1+\eta)(\tau_1+\tau_2)])^3}\cos\omega(\tau_1+2\tau_2)$$

$$+\frac{2(1+\eta)(1-\exp[-\gamma(1+\eta)\tau_2])\exp\{-[4\Gamma^*+\gamma(1+2\eta)]\tau_1-[\Gamma^*+\frac{1}{2}\gamma(1+3\eta)]\tau_2\}}{(1-\eta\exp[-\gamma(1+\eta)(\tau_1+\tau_2)])^3}\cos\omega(2\tau_1+\tau_2)\Bigg). \tag{36}$$

This expression does not reduce to Eq. (31) in the low temperature limit, since there the ground state population also decays with rate γ, while the ground state is stable here. Furthermore, the one-quantum coherences $|0\rangle\langle 1|$ and $|1\rangle\langle 2|$, that occur in Eq. (36), now decay in different ways [see Eq. (34)]. The term oscillating as $\cos\omega(2\tau_1+\tau_2)$ vanishes when the decay rates do not depend on the quantum states, as can be seen from the general expression in Appendix B. Hence, it is not present in Eqs. (29), (31), and (33). With state-dependent decay rates, the perfect destructive interference between different quantum mechanical pathways is partly destroyed, which yields this additional term to the response function that has not been reported before. This situation is analogous to that discussed by Fourkas *et al.*,[90] who showed that a harmonic oscillator, linearly coupled to a resonant optical field, can behave nonlinearly due to damping processes.

In addition to the homogeneous damping, discussed so far, inhomogeneity can be taken into account by considering a distribution of environments for the oscillator. This leads to a distribution $g(\omega)$ of oscillator frequencies, yielding the following nonlinear response functions

$$R^{(3)}_{\rm inh}(\tau_1)=\int_0^{+\infty}d\omega g(\omega)R^{(3)}(\omega,\tau_1), \tag{37a}$$

$$R^{(5)}_{\rm inh}(\tau_1,\tau_2)=\int_0^{+\infty}d\omega g(\omega)R^{(5)}(\omega,\tau_1,\tau_2), \tag{37b}$$

where $R^{(3)}(\omega,\tau_1)$ and $R^{(5)}(\omega,\tau_1,\tau_2)$ are given by Eqs. (28) and (29), Eqs. (30) and (31), or Eqs. (35) and (36), whatever the homogeneous dynamics is that applies to the situation. The general effect of inhomogeneous broadening is clear from Eqs. (37). The damping of all third-order and most fifth-order terms increases, due to the fact that a distribution of sin and cos functions beat against each other. The only exception is the $\cos\omega(\tau_1-\tau_2)$ term of the fifth-order response, which is insensitive to any distribution $g(\omega)$ for $\tau_1=\tau_2$. This fifth-order effect, which is based on macroscopic rephasing of coherent motion, therefore enables the experimental separation of homogeneous and inhomogeneous contributions to the nuclear spectrum. This is not possible in third-order response.

Whether rephasing is possible in a nonlinear experiment depends on the quantum mechanical pathway of propagation and the dynamics of the nuclear motion. The physics of the rephasing process can be illustrated by the Liouville space pathways of the system, that give rise to this special part of

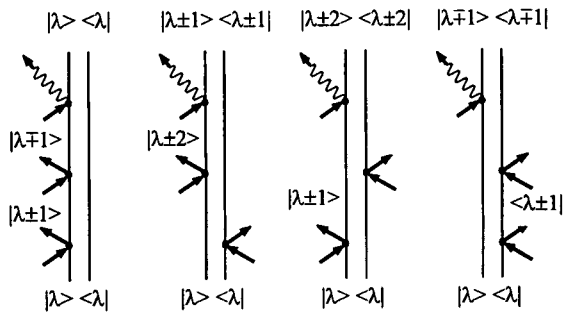

FIG. 6. The four Feynman diagrams that allow for rephasing in the inhomogeneous limit of nuclear dynamics. Due to the fact that in a harmonic ladder system the inhomogeneous distribution is correlated for the different transitions, dephasing on one transition can be compensated by rephasing on another one. For details consult the text.

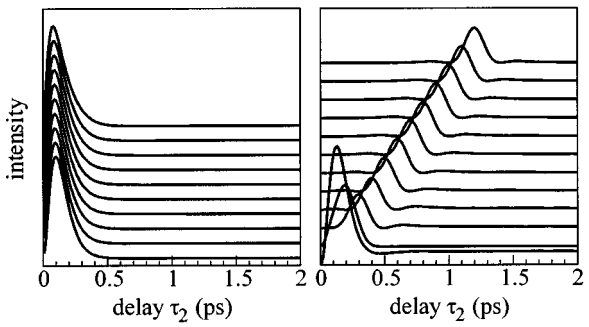

FIG. 7. The τ_2 dependence of the fifth-order response of a single-harmonic mode is calculated in the homogeneous (left) and inhomogeneous (right) limits. The value of τ_1 is 100 fs for the bottom traces, and increases in steps of 100 fs for each subsequent trace. The parameters of the calculations are given in the text. The curves for the homogeneous case have been rescaled to the same height.

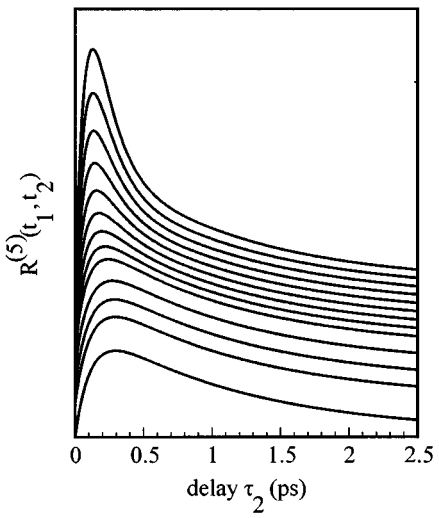

FIG. 8. Calculated fifth-order response for two independent harmonic modes as function of the propagation time τ_2, with τ_1 fixed at 100, 150, 200, 250, 300, 350, 400, 450, 500, 600, 700, 800 and 1000 fs (top to bottom). The underdamped mode, with a subpicosecond relaxation time, dominates the response at small τ_1. The response for τ_1 larger than 0.5 ps is completely determined by the overdamped mode, which decays on the much longer time scale of the diffusive response (~1.6 ps).

the total response. The corresponding Feynman diagrams are shown in Fig. 6. They are special cases of the general diagrams, shown as Figs. 5(d.1)–5(d.4). Initially a one-quantum transition creates a coherent superposition, e.g., $|\lambda\rangle\langle\lambda\pm1|$, and the system acquires a phase $\exp(\pm i\omega\tau_1)$ during the first propagation period. For a large inhomogeneous distribution of frequencies, the macroscopic phase coherence rapidly decays. The second interaction induces a two-quantum transition, which converts the system into the coherence $|\lambda\pm2\rangle\langle\lambda\pm1|$ or $|\lambda\rangle\langle\mp1|$. During the second propagation period, the system acquires the phase $\exp(\mp i\omega\tau_2)$. When τ_2 is equal to τ_1, the phases of the two propagation periods compensate for each other, independent of the particular frequency of the oscillator, and the macroscopic phase coherence is recovered, leading to a motional echo. When the inhomogeneous broadening is very small compared to the homogeneous broadening, the decay during the periods τ_1 and τ_2 is irreversible, and there is no motional echo. This demonstrates the unique information content of the fifth-order experiment compared with the third-order experiment.

To illustrate the sensitivity of the fifth-order response to the character of the nuclear dynamics, the response of a single-harmonic mode was calculated in the limits of purely homogeneous and inhomogeneous dephasing. This is shown in Fig. 7. For simplicity we assumed the homogeneous damping to be level independent. The central frequency and width of the third-order spectral response (full width at half-maximum) were taken to be 40 and 50 cm^{-1}, respectively, which are typical values for many molecular liquids, and in particular for CS_2.[75,76] In the homogeneous limit the amplitudes of the different curves have been rescaled to the same value in order to compare the position and the shape of the traces. The loss of macroscopic coherence is irreversible and hence the amplitude reaches its maximum always at the same propagation time τ_2, independent of the delay τ_1.

The situation is completely different when pure inhomogeneous broadening causes the same spectral width. The fifth-order response function in the static limit is given by Eq. (37b) with all homogeneous damping rates equal to zero [Eq. (29)]. The amplitudes of these traces have not been rescaled. After an initial rapid decay, the signal amplitude remains constant, irrespective of the value of the propagation time τ_1. The maximum occurs when τ_2 is equal to τ_1. This behavior results from the fact that dephasing due to a static distribution of frequencies is reversible. In the third-order response there is no difference between the two cases, because there are no contributions that are sensitive to the character of the dynamics. It is then simply the total spectral response that determines the response function.

C. Multiple modes

When there are several modes that determine the optical response, and there is no coupling between these modes, the total response functions are just the sum of all independent responses

$$R^{(3)}_{\mathrm{tot}}(\tau_1)=\sum_i R^{(3)}_i(\tau_1), \tag{38a}$$

$$R^{(5)}_{\mathrm{tot}}(\tau_1,\tau_2)=\sum_i R^{(5)}_i(\tau_1,\tau_2). \tag{38b}$$

Note that in Refs. 70, 73, and 77 the fifth-order response function was not calculated in this way, as a direct sum of mutually independent amplitudes. Instead, the modes seemed to be intrinsically coupled, in a way that we believe to be incorrect.[94]

In order to illustrate this, we performed model calculations for two harmonic modes, one underdamped and one overdamped. The parameters of the damping and frequency of the underdamped mode are the same as above, while the

overdamped mode simulates diffusive behavior with a decay constant $\tau_D=1.65$ ps and an exponential rise time decay $\tau_R=72$ fs.[76] For a ratio of $(\alpha_1)^2_{\mathrm{UD}}/(\alpha_1)^2_{\mathrm{OD}}=7.3$, these parameters model the third-order response of CS_2 in the homogeneous limit.[75,76] When the same ratio is assumed for the fifth-order contributions, the traces of Fig. 8 are calculated. It is clear that the fifth-order response for variable τ_2 changes shape as function of the delay time τ_1. For small τ_1 the response is dominated by the underdamped mode, while for big τ_1 the response is completely due to the overdamped mode. This change in shape is caused by the difference in the decay rates of the two modes. When the modes are intrinsically coupled, this is not correctly taken into account.[94]

In general, it is not possible to predict the fifth-order response from third-order measurements when more than one mode is involved in the coordinate dependent (hyper) polarizabilities, since the ratio of the various contributions is not known. The relative amplitude depends on the expansion coefficients of the polarizability operators in the coordinates of the modes. For the third-order response the lowest order in the nuclear response is determined by the coefficients α_1^2 [see Eqs. (28), (30), or (35)], while for the fifth-order response the lowest order contribution is determined by $\alpha_1^2\alpha_2$ [see Eqs. (29), (31), or (36)]. It is very unlikely that the same form of $\alpha(q)$ holds for modes as different as overdamped diffusion and coherent librations, such as were used in recent literature to describe higher-order optical response in liquids.[70–77] The ratio of the coefficients will therefore in general change with the order of the expansion of the polarizability. Hence, experimental results must be used to determine the relative importance of the different modes in different orders of nonlinear optical experiments.

IV. SUMMARY AND CONCLUSIONS

A unified theory of studies on nuclear dynamics by femtosecond electronically nonresonant four- and six-wave mixing was presented. The theoretical approach was based on the Born–Oppenheimer approximation, which allows one to eliminate the electrons from the description of the dynamics. The theory was formulated such that the nonlinear response functions are independent of the Hamiltonian of the system and the coordinate dependence of the (hyper) polarizabilities. The possible role of hyperpolarizabilities in higher-order Raman scattering experiments was stressed. These give rise to processes that contain the same dynamical information as lower order response. Serious misinterpretation of experimental data may result from such contributions to the nonlinear signals.

The theory was worked out in more detail for harmonic nuclear motion. Nonlinearity was introduced by expanding the (hyper) polarizabilities in the nuclear coordinate. Quadratic dependence is required to yield a fifth-order nonlinear response. Damping was treated in the weak coupling limit using level-independent and level-dependent damping parameters. The results were compared to a Brownian oscillator model for the bath. For level-dependent damping we found that all contributions to the third- and fifth-order response functions become temperature dependent. The decays increase with temperature. Also, an additional contribution to the fifth-order response was found, caused by the fact that the destructive interference between different quantum mechanical pathways is destroyed by the level-dependent damping.

In contrast to the third-order response, the fifth-order response is sensitive to dephasing mechanisms of the induced nuclear motion. The reason is that there are two independent propagation times in the process, which allows for rephasing of macroscopic coherence when dephasing is caused by a static distribution of transition frequencies. This leads to a motional echo, when the two propagation times are equal. In the homogeneous limit the fifth-order response as function of the second propagation time always has approximately the same shape and position, independent of the first propagation time. This is due to the fact that the dephasing in the homogeneous limit is irreversible.

When two or more modes are involved in the nonlinear optical response of the medium, the situation becomes more complex. The relative magnitudes of the modes in third- and fifth-order response are in general not correlated. They have to be determined from experiment. Model calculations were used to show that the fifth-order response changes its shape, when two independent modes have different homogeneous damping parameters.

Experimental six-wave mixing results will be reported in a subsequent paper.[76] The theory, presented here, will be employed then to analyze the two-dimensional response, generated through three subsequent, temporally well separated Rayleigh/Raman scattering events. The main problem, experimentally, is to separate these processes from other contributions, such as the fifth-order effects due to hyperpolarizabilities, depicted in Fig. 4, or fifth-order response that is due to two subsequent third-order scattering events. It will be shown that a proper choice of polarization—and phase matching conditions is crucial to the proper identification of the two-dimensional signals.

ACKNOWLEDGMENTS

T.S. and K.D. thank M. Besnard, J. Knoester, and C. Sourisseau for discussions, and are grateful to A. Tokmakoff and K. Tominaga for discussions and sending preprints prior to publication. The investigations were supported by the Netherlands Foundation for Physical Research (FOM) with financial aid from the Netherlands Organization for the Advancement of Science (NWO). J.T.F. thanks the Camille and Henry Dreyfus Foundation for a New Faculty Award, and the NSF for Grant No. CHE-9501598.

APPENDIX A: THE FIFTH-ORDER RESPONSE FUNCTION IN THE BOA

The fifth-order response function within the Born–Oppenheimer approximation, for electronically nonresonant

optical fields, is given by 32 independent terms. These originate from the perturbative expansion Eq. (16). The number of nuclear propagation periods varies from zero for the instantaneous electronic polarization (A1), to five for resonant FIR six-wave mixing experiments [term (A32)]. The processes with one to four propagation times (A2)–(A31) are due to combinations of (hyper-) Raman interactions and/or dipole transitions, governed by the (hyper) polarizability operators $\alpha_{ij}, \beta_{ijk}, \gamma_{ijkl}, \epsilon_{ijklm}$ and the dipole moment operator m_i

$$
\begin{aligned}
&R^{(5)}_{ijklnm}(t,t_1,t_2,t_3,t_4,t_5) \\
&\quad = \langle \zeta_{ijklmn} \rangle \delta(t-t_1)\delta(t_1-t_2)\delta(t_2-t_3)\delta(t_3-t_4)\delta(t_4-t_5) && \text{(A1)} \\
&\qquad + \frac{i}{\hbar}\langle [\widetilde{m}_i(t), \tfrac{1}{5}\widetilde{\epsilon}_{jklmn}(t_1)]\rangle \delta(t_1-t_2)\delta(t_2-t_3)\delta(t_3-t_4)\delta(t_4-t_5)H(t-t_1) && \text{(A2)} \\
&\qquad + \frac{i}{\hbar}\langle [\widetilde{\alpha}_{ij}(t), \tfrac{1}{4}\widetilde{\gamma}_{klmn}(t_2)]\rangle \delta(t-t_1)\delta(t_2-t_3)\delta(t_3-t_4)\delta(t_4-t_5)H(t_1-t_2) && \text{(A3)} \\
&\qquad + \frac{i}{\hbar}\langle [\widetilde{\beta}_{ijk}(t), \tfrac{1}{3}\widetilde{\beta}_{lmn}(t_3)]\rangle \delta(t-t_1)\delta(t_1-t_2)\delta(t_3-t_4)\delta(t_4-t_5)H(t_2-t_3) && \text{(A4)} \\
&\qquad + \frac{i}{\hbar}\langle [\widetilde{\gamma}_{ijkl}(t), \tfrac{1}{2}\widetilde{\alpha}_{mn}(t_4)]\rangle \delta(t-t_1)\delta(t_1-t_2)\delta(t_2-t_3)\delta(t_4-t_5)H(t_3-t_4) && \text{(A5)} \\
&\qquad + \frac{i}{\hbar}\langle [\widetilde{\epsilon}_{ijklm}(t), \widetilde{m}_n(t_5)]\rangle \delta(t-t_1)\delta(t_1-t_2)\delta(t_2-t_3)\delta(t_3-t_4)H(t_4-t_5) && \text{(A6)} \\
&\qquad + \left(\frac{i}{\hbar}\right)^2 \langle [[\widetilde{m}_i(t), \widetilde{m}_j(t_1)], \tfrac{1}{4}\widetilde{\gamma}_{klmn}(t_2)]\rangle \delta(t_2-t_3)\delta(t_3-t_4)\delta(t_4-t_5)H(t-t_1)H(t_1-t_2) && \text{(A7)} \\
&\qquad + \left(\frac{i}{\hbar}\right)^2 \langle [[\widetilde{m}_i(t), \tfrac{1}{2}\widetilde{\alpha}_{jk}(t_1)], \tfrac{1}{3}\widetilde{\beta}_{lmn}(t_3)]\rangle \delta(t_1-t_2)\delta(t_3-t_4)\delta(t_4-t_5)H(t-t_1)H(t_2-t_3) && \text{(A8)} \\
&\qquad + \left(\frac{i}{\hbar}\right)^2 \langle [[\widetilde{m}_i(t), \tfrac{1}{3}\widetilde{\beta}_{jkl}(t_1)], \tfrac{1}{2}\widetilde{\alpha}_{mn}(t_4)]\rangle \delta(t_1-t_2)\delta(t_2-t_3)\delta(t_4-t_5)H(t-t_1)H(t_3-t_4) && \text{(A9)} \\
&\qquad + \left(\frac{i}{\hbar}\right)^2 \langle [[\widetilde{m}_i(t), \tfrac{1}{4}\widetilde{\gamma}_{jklm}(t_1)], \widetilde{m}_n(t_5)]\rangle \delta(t_1-t_2)\delta(t_2-t_3)\delta(t_3-t_4)H(t-t_1)H(t_4-t_5) && \text{(A10)} \\
&\qquad + \left(\frac{i}{\hbar}\right)^2 \langle [[\widetilde{\alpha}_{ij}(t), \widetilde{m}_k(t_2)], \widetilde{\beta}_{lmn}(t_3)]\rangle \delta(t-t_1)\delta(t_3-t_4)\delta(t_4-t_5)H(t_1-t_2)H(t_2-t_3) && \text{(A11)} \\
&\qquad + \left(\frac{i}{\hbar}\right)^2 \langle [[\widetilde{\alpha}_{ij}(t), \tfrac{1}{2}\widetilde{\alpha}_{kl}(t_2)], \tfrac{1}{2}\widetilde{\alpha}_{mn}(t_4)]\rangle \delta(t-t_1)\delta(t_2-t_3)\delta(t_4-t_5)H(t_1-t_2)H(t_3-t_4) && \text{(A12)} \\
&\qquad + \left(\frac{i}{\hbar}\right)^2 \langle [[\widetilde{\alpha}_{ij}(t), \tfrac{1}{3}\widetilde{\beta}_{klm}(t_2)], \widetilde{m}_n(t_5)]\rangle \delta(t-t_1)\delta(t_2-t_3)\delta(t_3-t_4)H(t_1-t_2)H(t_4-t_5) && \text{(A13)} \\
&\qquad + \left(\frac{i}{\hbar}\right)^2 \langle [[\widetilde{\beta}_{ijk}(t), \widetilde{m}_l(t_3)], \tfrac{1}{2}\widetilde{\alpha}_{mn}(t_4)]\rangle \delta(t-t_1)\delta(t_1-t_2)\delta(t_4-t_5)H(t_2-t_3)H(t_3-t_4) && \text{(A14)} \\
&\qquad + \left(\frac{i}{\hbar}\right)^2 \langle [[\widetilde{\beta}_{ijk}(t), \tfrac{1}{2}\widetilde{\alpha}_{lm}(t_3)], \widetilde{m}_n(t_5)]\rangle \delta(t-t_1)\delta(t_1-t_2)\delta(t_3-t_4)H(t_2-t_3)H(t_4-t_5) && \text{(A15)} \\
&\qquad + \left(\frac{i}{\hbar}\right)^2 \langle [[\widetilde{\gamma}_{ijkl}(t), \widetilde{m}_m(t_4)], \widetilde{m}_n(t_5)]\rangle \delta(t-t_1)\delta(t_1-t_2)\delta(t_2-t_3)H(t_3-t_4)H(t_4-t_5) && \text{(A16)} \\
&\qquad + \left(\frac{i}{\hbar}\right)^3 \langle [[[\widetilde{m}_i(t), \widetilde{m}_j(t_1)], \widetilde{m}_k(t_2)], \tfrac{1}{3}\widetilde{\beta}_{lmn}(t_3)]\rangle \delta(t_3-t_4)\delta(t_4-t_5)H(t-t_1)H(t_1-t_2)H(t_2-t_3) && \text{(A17)} \\
&\qquad + \left(\frac{i}{\hbar}\right)^3 \langle [[[\widetilde{m}_i(t), \widetilde{m}_j(t_1)], \tfrac{1}{2}\widetilde{\alpha}_{kl}(t_2)], \tfrac{1}{2}\widetilde{\alpha}_{mn}(t_4)]\rangle \delta(t_2-t_3)\delta(t_4-t_5)H(t-t_1)H(t_1-t_2)H(t_3-t_4) && \text{(A18)}
\end{aligned}
$$

$$+\left(\frac{i}{\hbar}\right)^3\langle[[[\tilde{m}_i(t),\tilde{m}_j(t_1)],\tfrac{1}{3}\tilde{\beta}_{klm}(t_2)],\tilde{m}_n(t_5)]\rangle\,\delta(t_2-t_3)\,\delta(t_3-t_4)H(t-t_1)H(t_1-t_2)H(t_4-t_5) \tag{A19}$$

$$+\left(\frac{i}{\hbar}\right)^3\langle[[[\tilde{m}_i(t),\tfrac{1}{2}\tilde{\alpha}_{jk}(t_1)],\tilde{m}_l(t_3)],\tfrac{1}{2}\tilde{\alpha}_{mn}(t_4)]\rangle\,\delta(t_1-t_2)\,\delta(t_4-t_5)H(t-t_1)H(t_2-t_3)H(t_3-t_4) \tag{A20}$$

$$+\left(\frac{i}{\hbar}\right)^3\langle[[[\tilde{m}_i(t),\tfrac{1}{2}\tilde{\alpha}_{jk}(t_1)],\tfrac{1}{2}\tilde{\alpha}_{lm}(t_3)],\tilde{m}_n(t_5)]\rangle\,\delta(t_1-t_2)\,\delta(t_4-t_5)H(t-t_1)H(t_2-t_3)H(t_4-t_5) \tag{A21}$$

$$+\left(\frac{i}{\hbar}\right)^3\langle[[[\tilde{m}_i(t),\tfrac{1}{3}\tilde{\beta}_{jkl}(t_1)],\tilde{m}_m(t_4)],\tilde{m}_n(t_5)]\rangle\,\delta(t_1-t_2)\,\delta(t_2-t_3)H(t-t_1)H(t_3-t_4)H(t_4-t_5) \tag{A22}$$

$$+\left(\frac{i}{\hbar}\right)^3\langle[[[\tilde{\alpha}_{ij}(t),\tilde{m}_k(t_2)],\tilde{m}_l(t_3)],\tfrac{1}{2}\tilde{\alpha}_{mn}(t_4)]\rangle\,\delta(t-t_1)\,\delta(t_4-t_5)H(t_1-t_2)H(t_2-t_3)H(t_3-t_4) \tag{A23}$$

$$+\left(\frac{i}{\hbar}\right)^3\langle[[[\tilde{\alpha}_{ij}(t),\tilde{m}_k(t_2)],\tfrac{1}{2}\tilde{\alpha}_{lm}(t_3)],\tilde{m}_n(t_5)]\rangle\,\delta(t-t_1)\,\delta(t_3-t_4)H(t_1-t_2)H(t_2-t_3)H(t_4-t_5) \tag{A24}$$

$$+\left(\frac{i}{\hbar}\right)^3\langle[[[\tilde{\alpha}_{ij}(t),\tfrac{1}{2}\tilde{\alpha}_{kl}(t_2)],\tilde{m}_m(t_4)],\tilde{m}_n(t_5)]\rangle\,\delta(t-t_1)\,\delta(t_2-t_3)H(t_1-t_2)H(t_3-t_4)H(t_4-t_5) \tag{A25}$$

$$+\left(\frac{i}{\hbar}\right)^3\langle[[[\tilde{\beta}_{ijk}(t),\tilde{m}_l(t_3)],\tilde{m}_m(t_4)],\tilde{m}_n(t_5)]\rangle\,\delta(t-t_1)\,\delta(t_1-t_2)H(t_2-t_3)H(t_3-t_4)H(t_4-t_5) \tag{A26}$$

$$+\left(\frac{i}{\hbar}\right)^4\langle[[[[\tilde{m}_i(t),\tilde{m}_j(t_1)],\tilde{m}_k(t_2)],\tilde{m}_l(t_3)],\tfrac{1}{2}\tilde{\alpha}_{mn}(t_4)]\rangle\,\delta(t_4-t_5)H(t-t_1)H(t_1-t_2)H(t_2-t_3)H(t_3-t_4) \tag{A27}$$

$$+\left(\frac{i}{\hbar}\right)^4\langle[[[[\tilde{m}_i(t),\tilde{m}_j(t_1)],\tilde{m}_k(t_2)],\tfrac{1}{2}\tilde{\alpha}_{lm}(t_3)],\tilde{m}_n(t_5)]\rangle\,\delta(t_3-t_4)H(t-t_1)H(t_1-t_2)H(t_2-t_3)H(t_4-t_5) \tag{A28}$$

$$+\left(\frac{i}{\hbar}\right)^4\langle[[[[\tilde{m}_i(t),\tilde{m}_j(t_1)],\tfrac{1}{2}\tilde{\alpha}_{kl}(t_2)],\tilde{m}_m(t_4)],\tilde{m}_n(t_5)]\rangle\,\delta(t_2-t_3)H(t-t_1)H(t_1-t_2)H(t_3-t_4)H(t_4-t_5) \tag{A29}$$

$$+\left(\frac{i}{\hbar}\right)^4\langle[[[[\tilde{m}_i(t),\tfrac{1}{2}\tilde{\alpha}_{jk}(t_1)],\tilde{m}_l(t_3)],\tilde{m}_m(t_4)],\tilde{m}_n(t_5)]\rangle\,\delta(t_1-t_2)H(t-t_1)H(t_2-t_3)H(t_3-t_4)H(t_4-t_5) \tag{A30}$$

$$+\left(\frac{i}{\hbar}\right)^4\langle[[[[\tilde{\alpha}_{ij}(t),\tilde{m}_k(t_2)],\tilde{m}_l(t_3)],\tilde{m}_m(t_4)],\tilde{m}_n(t_5)]\rangle\,\delta(t-t_1)H(t_1-t_2)H(t_2-t_3)H(t_3-t_4)H(t_4-t_5) \tag{A31}$$

$$+\left(\frac{i}{\hbar}\right)^5\langle\{[[[[\tilde{m}_i(t),\tilde{m}_j(t_1)],\tilde{m}_k(t_2)],\tilde{m}_l(t_3)],\tilde{m}_m(t_4)],\tilde{m}_n(t_5)\}\rangle H(t-t_1)H(t_1-t_2)H(t_2-t_3)H(t_3-t_4)H(t_4-t_5). \tag{A32}$$

APPENDIX B: HARMONIC THIRD- AND FIFTH-ORDER NONLINEAR RESPONSE FUNCTIONS

The nuclear part of the nonlinear response functions can be written explicitly in terms of the harmonic oscillator states $|\lambda>$ by expanding the electronic (hyper) polarizabilities in the nuclear coordinate q, and using the matrix elements Eq. (27) on the general response functions Eqs. (25) and (26). The third-and fifth-order nonlinear response functions in this representation are:

$$R^{(3)}(\tau_1)=\langle\gamma\rangle\,\delta(\tau_1)-\frac{\alpha_1^2}{2m\omega}\sin\,\omega\tau_1\sum_\lambda\,P(\lambda)[\lambda e^{-\Gamma_{\lambda,\lambda-1}\tau_1}-(\lambda+1)e^{-\Gamma_{\lambda,\lambda+1}\tau_1}]$$

$$-\frac{\alpha_2^2\hbar}{(2m\omega)^2}\sin 2\omega\tau_1\sum_\lambda\,P(\lambda)[\lambda(\lambda-1)e^{-\Gamma_{\lambda,\lambda-2}\tau_1}-(\lambda+1)(\lambda+2)e^{-\Gamma_{\lambda,\lambda+2}\tau_1}],$$

$$R^{(5)}(\tau_1,\tau_2)=\langle\zeta\rangle\,\delta(\tau_1)\,\delta(\tau_2)-\frac{\alpha_1\gamma_1}{2m\omega}\left(\frac{1}{2}\,\delta(\tau_1)\sin\,\omega_{\lambda\mu}\tau_2\sum_\lambda\,P(\lambda)[\lambda e^{-\Gamma_{\lambda,\lambda-1}\tau_2}-(\lambda+1)e^{-\Gamma_{\lambda,\lambda+1}\tau_2}]\right.$$

$$\left.+\,\delta(\tau_2)\sin\,\omega_{\lambda\mu}\tau_1\sum_\lambda\,P(\lambda)[\lambda e^{-\Gamma_{\lambda,\lambda-1}\tau_1}-(\lambda+1)e^{-\Gamma_{\lambda,\lambda+1}\tau_1}]\right)$$

$$
\begin{aligned}
&- \frac{\alpha_2^3\hbar}{2(2m\omega)^3}\Bigg(\cos 2\omega(\tau_1+\tau_2)\sum_\lambda P(\lambda)[(4\lambda^2+12\lambda+8)e^{-\Gamma_{\lambda,\lambda+2}(\tau_1+\tau_2)}+(-4\lambda^2+4\lambda)e^{-\Gamma_{\lambda,\lambda-2}(\tau_1+\tau_2)}] \\
&+\cos 2\omega\tau_1\sum_\lambda P(\lambda)[(2\lambda^3-\lambda^2-\lambda)e^{-\Gamma_{\lambda,\lambda-2}\tau_1-\Gamma_{\lambda,\lambda}\tau_2}+(-2\lambda^3+5\lambda^2-3\lambda)e^{-\Gamma_{\lambda,\lambda-2}\tau_1-\Gamma_{\lambda-2,\lambda-2}\tau_2} \\
&+(2\lambda^3+7\lambda^2+7\lambda+2)e^{-\Gamma_{\lambda,\lambda+2}\tau_1-\Gamma_{\lambda,\lambda}\tau_2}+(-2\lambda^3-11\lambda^2-19\lambda-10)e^{-\Gamma_{\lambda,\lambda+2}\tau_1-\Gamma_{\lambda+2,\lambda+2}\tau_2}]\Bigg) \\
&- \frac{\alpha_1^2\alpha_2}{2(2m\omega)^2}\Bigg(\cos\omega(\tau_1-\tau_2)\sum_\lambda P(\lambda)[(\lambda^2+\lambda)e^{-\Gamma_{\lambda,\lambda+1}\tau_1-\Gamma_{\lambda,\lambda-1}\tau_2}+(\lambda^2+\lambda)e^{-\Gamma_{\lambda,\lambda-1}\tau_1-\Gamma_{\lambda,\lambda+1}\tau_2} \\
&+(-\lambda^2+\lambda)e^{-\Gamma_{\lambda,\lambda-1}\tau_1-\Gamma_{\lambda-1,\lambda-2}\tau_2}+(-\lambda^2-3\lambda-2)e^{-\Gamma_{\lambda,\lambda+1}\tau_1-\Gamma_{\lambda+1,\lambda+2}\tau_2}] \\
&+\cos\omega(\tau_1+\tau_2)\sum_\lambda P(\lambda)[(2\lambda^2-\lambda)e^{-\Gamma_{\lambda,\lambda-1}(\tau_1+\tau_2)}+(-2\lambda^2-\lambda)e^{-\Gamma_{\lambda,\lambda-1}(\tau_1+\tau_2)} \\
&+(2\lambda^2+5\lambda+3)e^{-\Gamma_{\lambda,\lambda+1}(\tau_1+\tau_2)}+(-2\lambda^2-3\lambda-1)e^{-\Gamma_{\lambda,\lambda+1}(\tau_1+\tau_2)}] \\
&+\cos\omega\tau_1\sum_\lambda P(\lambda)[(2\lambda^2+\lambda)e^{-\Gamma_{\lambda,\lambda-1}\tau_1-\Gamma_{\lambda,\lambda}\tau_2}+(-2\lambda^2+\lambda)e^{-\Gamma_{\lambda,\lambda-1}\tau_1-\Gamma_{\lambda-1,\lambda-1}\tau_2} \\
&+(2\lambda^2+3\lambda+1)e^{-\Gamma_{\lambda,\lambda+1}\tau_1-\Gamma_{\lambda,\lambda}\tau_2}+(-2\lambda^2-5\lambda-3)e^{-\Gamma_{\lambda,\lambda+1}\tau_1-\Gamma_{\lambda+1,\lambda+1}\tau_2}] \\
&+\cos\omega(\tau_1+2\tau_2)\sum_\lambda P(\lambda)[(\lambda^2-\lambda)e^{-\Gamma_{\lambda,\lambda-1}\tau_1-\Gamma_{\lambda,\lambda-2}\tau_2}+(\lambda^2+3\lambda+2)e^{-\Gamma_{\lambda,\lambda+1}\tau_1-\Gamma_{\lambda,\lambda+2}\tau_2} \\
&+(-\lambda^2-\lambda)e^{-\Gamma_{\lambda,\lambda+1}\tau_1-\Gamma_{\lambda+1,\lambda-1}\tau_2}+(-\lambda^2-\lambda)e^{-\Gamma_{\lambda,\lambda-1}\tau_1-\Gamma_{\lambda+1,\lambda-1}\tau_2}] \\
&+\cos\omega(2\tau_1+\tau_2)\sum_\lambda P(\lambda)[(\lambda^2-\lambda)e^{-\Gamma_{\lambda,\lambda-2}\tau_1-\Gamma_{\lambda,\lambda-1}\tau_2}+(-\lambda^2-3\lambda-2)e^{-\Gamma_{\lambda,\lambda+2}\tau_1-\Gamma_{\lambda+1,\lambda+2}\tau_2} \\
&+(\lambda^2+3\lambda+2)e^{-\Gamma_{\lambda,\lambda+2}\tau_1-\Gamma_{\lambda+1,\lambda}\tau_2}+(-\lambda^2+\lambda)e^{-\Gamma_{\lambda,\lambda-2}\tau_1-\Gamma_{\lambda-1,\lambda-2}\tau_2}]\Bigg).
\end{aligned}
$$

The Feynman diagrams Figs. 3 and 5 are pictorial representations of the system propagation, that give rise to these expressions. $P(\lambda)$ is the initial thermal distribution over the harmonic quantum states $|\lambda\rangle$. Both upward and downward transitions are induced by the optical fields. Damping was introduced in this picture in the weak coupling limit, by writing complex transition frequencies according to the substitution $\omega_{\lambda\mu}\rightarrow\omega_{\lambda\mu}+i\Gamma_{\lambda\mu}$. The damping parameter $\Gamma_{\lambda\mu}$ in principle contains contributions from the lifetimes $\gamma_{\lambda,\mu}$ of states $|\lambda\rangle$ and $|\mu\rangle$, and of pure dephasing processes $\Gamma^*_{\lambda\mu}$ that modulate the transition frequency between both states: $\Gamma_{\lambda\mu}=\frac{1}{2}(\gamma_\lambda+\gamma_\mu)+\Gamma^*_{\lambda\mu}$.

The nonlinear response functions can be further evaluated in different limits of the system dynamics. For undamped oscillators ($\Gamma_{\lambda\mu}=0$), Eqs. (28) and (29) result, while for state independent damping [$\gamma\equiv\gamma_\lambda=\gamma_\mu$, $\Gamma_1\equiv\Gamma_{\lambda\mu}\delta(\lambda,\mu\pm1)$, $\Gamma_2\equiv\Gamma_{\lambda\mu}\delta(\lambda,\mu\pm2)$] the relaxation functions are given by Eqs. (30) and (31). In a more microscopic approach, the harmonic oscillator is explicitly coupled to a heat bath. For linear coupling with a harmonic heat bath, the transition rate from state $|\lambda\rangle$ to state $|\lambda-1\rangle$ acquires a quantum number dependence,[90–93] which can be written as $k_{\lambda\rightarrow\lambda-1}=\lambda\gamma$. Here γ is the rate down out of the first excited state $|1\rangle$. Quadratic coupling leads to a quantum number dependence of the dephasing rate,[90–93] which can be written as $\Gamma^*_{\lambda\mu}=(\lambda-\mu)^2\Gamma^*$, where Γ^* is the one-quantum dephasing rate.

For a thermally activated system ($kT\geqslant\hbar\omega$), next to downward transitions also upward transitions have to be considered. In steady state, all populations $n(\lambda)$ are time independent, which leads to relations among the transition rates. For instance, for the ground state population $n(0)$ it is found that $dn(0)/dt=-k_{0\rightarrow1}n(0)+k_{1\rightarrow0}n(1)=0$. It follows that $k_{0\rightarrow1}=k_{1\rightarrow0}\eta=\gamma\eta$, where η is the Boltzmann factor $\eta\equiv\exp(-\hbar\omega/kT)$. Iterative application of this detailed balance argument gives for the upward transitions the quantum number dependence $k_{\lambda\rightarrow\lambda+1}=(\lambda+1)\gamma\eta$. The total population decay rate out of state $|\lambda\rangle$ is the sum of the upward and downward rates: $\gamma_\lambda=\lambda\gamma+(\lambda+1)\gamma\eta$. When this quantum number dependence of the population decay and that of the dephasing rate are used for the damping parameters $\Gamma_{\lambda\mu}$, Eq. (34) results. The third- and fifth-order response functions above can then be evaluated by writing the initial thermal distribution as $P(\lambda)=e^{-\hbar\omega\lambda/kt}/\Sigma_\lambda(e^{-\hbar\omega\lambda/kT})=\eta^\lambda(1-\eta)$. The sums over λ, that occur in the expressions for $R^{(3)}(\tau_1)$ and $R^{(5)}(\tau_1,\tau_2)$, can be evaluated in terms of (the derivatives

of) geometric sums, which then gives the nonlinear response functions Eqs. (35) and (36).

[1] R. J. Jimenez, G. R. Fleming, P. V. Kumar, and M. Maroncelli, Nature **369**, 471 (1994).
[2] P. Hänggi, P. Talkner, and M. Borkovec, Rev. Mod. Phys. **62**, 251 (1990).
[3] W. G. Rothschild, J. Soussen-Jacob, J. Bessière, and J. Vincent-Geisse, J. Chem. Phys. **79**, 3002 (1983).
[4] E. Zoïdis, M. Besnard, and J. Yarwood, Chem. Phys. **196**, 521 (1995).
[5] P. A. Madden, in *Ultrafast Phenomena IV*, edited by D. A. Auston and K. B. Eisenthal (Springer, Berlin, 1984), p. 244.
[6] W. G. Rothschild, R. M. Cavagnat, and P. Maraval, J. Chem. Phys. **99**, 8922 (1993).
[7] N. Pesce da Silveira, H. Stassen, and Th. Dorfmüller, J. Chem. Phys. **101**, 9370 (1994).
[8] Y. Wang and Y. Tominaga, J. Chem. Phys. **101**, 3453 (1994).
[9] J. S. Friedman, M. C. Lee, and C. Y. She, Chem. Phys. Lett. **186**, 161 (1991).
[10] J. S. Friedman and C. Y. She, J. Chem. Phys. **99**, 4960 (1993).
[11] C. E. Barker, R. Trebino, A. G. Kostenbauder, and A. E. Siegman, J. Chem. Phys. **92**, 4740 (1990).
[12] D. Wang and G. Rivoire, J. Chem. Phys. **98**, 9279 (1993).
[13] G. Rivoire and D. Wang, J. Chem. Phys. **99**, 9460 (1993).
[14] Y.-X. Yan and K. A. Nelson, J. Chem. Phys. **87**, 6240 (1987).
[15] Y.-X. Yan and K. A. Nelson, J. Chem. Phys. **87**, 6257 (1987).
[16] S. Ruhman, A. G. Joly, and K. A. Nelson, IEEE J. Quantum Electron. **QE-14**, 460 (1988).
[17] S. Ruhman, B. Kohler, A. G. Joly, and K. A. Nelson, IEEE J. Quantum Electron. **QE-14**, 470 (1988).
[18] T. Hattori and T. Kobayashi, J. Chem. Phys. **94**, 3332 (1991).
[19] B. I. Greene, P. A. Fleury, H. L. Carter, and R. C. Farrow, Phys. Rev. A **29**, 471 (1984).
[20] D. McMorrow, W. T. Lotshaw, and G. A. Kenney-Wallace, IEEE J. Quantum Electron. **QE-24**, 443 (1988).
[21] D. McMorrow and W. T. Lotshaw, J. Phys. Chem. **95**, 10395 (1991).
[22] D. McMorrow and W. T. Lotshaw, Chem. Phys. Lett. **201**, 369 (1993).
[23] M. Cho, M. Du, N. F. Scherer, G. R. Fleming, and S. Mukamel, J. Chem. Phys. **99**, 2410 (1993).
[24] Y. J. Chang and E. W. Castner, J. Phys. Chem. **98**, 9712 (1994).
[25] S. Palese, L. Schilling, R. J. D. Miller, P. R. Staver, and W. T. Lotshaw, J. Phys. Chem. **98**, 6308 (1994).
[26] I. Santa, P. Foggi, R. Righini, and J. H. Williams, J. Phys. Chem. **98**, 7692 (1994).
[27] S. Ruhman, L. R. Williams, A. G. Joly, and K. A. Nelson, J. Phys. Chem. **91**, 2237 (1987).
[28] J. Etchepare, G. Grillon, J. P. Chambaret, G. Harmoniaux, and A. Orszag, Opt. Commun. **63**, 329 (1987).
[29] S. Ruhman and K. A. Nelson, J. Chem. Phys. **94**, 859 (1991).
[30] A. Waldman, U. Banin, E. Rabani, and S. Ruhman, J. Phys. Chem. **96**, 10842 (1992).
[31] A. Sengupta and M. D. Fayer, J. Chem. Phys. **100**, 1673 (1994).
[32] P. Vöhringer and N. F. Scherer, J. Phys. Chem. **99**, 2684 (1995).
[33] R. W. Hellwarth, Progr. Quant. Electron. **5**, 1 (1977).
[34] S. Kinoshita, Y. Kai, M. Yamaguchi, and T. Yagi, Phys. Rev. Lett. **75**, 148 (1995).
[35] M. G. Giorgini, P. Foggi, R. S. Cataliotti, M. R. Distefano, A. Morresi, and L. Mariani, J. Chem. Phys. **102**, 8763 (1995).
[36] P. Cong, J. D. Simon, and C. Y. She, J. Chem. Phys. **104**, 962 (1996).
[37] D. Frenkel and J. P. McTague, J. Chem. Phys. **72**, 2801 (1980).
[38] P. A. Madden and D. Kivelson, Adv. Chem. Phys. **56**, 467 (1984).
[39] L. C. Geiger and B. M. Ladanyi, J. Chem. Phys. **87**, 191 (1987).
[40] P. Debye, *Polar Molecules* (Dover, New York, 1929).
[41] J. McConnell, *Rotational Brownian Motion and Dielectric Theory* (Academic, London, 1980).
[42] N. E. Hill, Proc. Phys. Soc. (London) **82**, 723 (1963).
[43] S. K. Deb, Chem. Phys. **120**, 225 (1988).
[44] W. T. Coffey, Proc. R. Soc. London Ser. A **425**, 169 (1989).
[45] A. Polimeno, G. J. Moro, and J. H. Freed, J. Chem. Phys. **102**, 8094 (1995).
[46] B. C. Xu and R. M. Stratt, J. Chem. Phys. **92**, 1923 (1990).
[47] T. M. Wu and R. M. Loring, J. Chem. Phys. **97**, 8568 (1992).
[48] M. Cho, G. R. Fleming, S. Saito, I. Ohmine, and R. M. Stratt, J. Chem. Phys. **100**, 6672 (1994).
[49] P. Moore, A. Tokmakoff, T. Keyes, and M. D. Fayer, J. Chem. Phys. **103**, 3325 (1995).
[50] G. Seeley, T. Keyes, and B. Madan, J. Chem. Phys. **95**, 3847 (1991).
[51] M. Buchner, B. M. Ladanyi, and R. M. Stratt, J. Chem. Phys. **97**, 8522 (1992).
[52] R. Kubo, Adv. Chem. Phys. **15**, 101 (1969).
[53] S. Mukamel, Adv. Chem. Phys. **70**, 165 (1988).
[54] E. T. J. Nibbering, K. Duppen, and D. A. Wiersma, J. Chem. Phys. **93**, 5477 (1990).
[55] R. G. Gordon, J. Chem. Phys. **43**, 1307 (1965).
[56] R. F. Loring and S. Mukamel, J. Chem. Phys. **83**, 2116 (1985).
[57] H. Graener, G. Seifert, and A. Lauberau, Chem. Phys. Lett. **172**, 435 (1990).
[58] H. J. Bakker, P.C.M. Planken, and A. Lagendijk, Nature **347**, 745 (1990).
[59] D. Zimdars, A. Tokmakoff, S. Chen, S. R. Greenfield, M. D. Fayer, T. I. Smith, and H. A. Schwettman, Phys. Rev. Lett. **70**, 2718 (1993).
[60] A. Tokmakoff and M. D. Fayer, J. Chem. Phys. **103**, 2810 (1995).
[61] S. Bratos and J.-C. Leicknam, J. Chem. Phys. **103**, 4887 (1995).
[62] D. Vanden Bout, L. J. Muller, and M. Berg, Phys. Rev. Lett. **43**, 3700 (1991).
[63] L. J. Muller, D. Vanden Bout, and M. Berg, J. Chem. Phys. **99**, 810 (1993).
[64] R. Inaba, K. Tominaga, M. Tasumi, K. A. Nelson, and K. Yoshihara, Chem. Phys. Lett. **211**, 183 (1993).
[65] Y. Tanimura and S. Mukamel, J. Chem. Phys. **99**, 9496 (1993).
[66] R. P. Feynman and F. L. Vernon, Ann. Phys. **24**, 118 (1963).
[67] Y. Tanimura and S. Mukamel, Phys. Rev. E **47**, 118 (1993).
[68] J. A. Leegwater and S. Mukamel, J. Chem. Phys. **102**, 2365 (1995).
[69] V. Khidekel and S. Mukamel, Chem. Phys. Lett. **240**, 304 (1995).
[70] K. Tominaga and K. Yoshihara, Phys. Rev. Lett. **74**, 3061 (1995).
[71] K. Tominaga, G. P. Keogh, Y. Naitoh, and K. Yoshihara, J. Raman Spectrosc. **26**, 495 (1995).
[72] K. Tominaga and K. Yoshihara, J. Chem. Phys. **104**, 1159 (1996).
[73] K. Tominaga and K. Yoshihara, J. Chem. Phys. **104**, 4419 (1996).
[74] T. Steffen and K. Duppen, in *Femtochemistry II*, edited by M. Chergui (World Scientific, Singapore, 1996), p. 583.
[75] T. Steffen and K. Duppen, Phys. Rev. Lett. **76**, 1224 (1996).
[76] T. Steffen and K. Duppen (unpublished).
[77] S. Palese, J. T. Buontempo, L. Schilling, W. T. Lotshaw, Y. Tanimura, S. Mukamel, and R. J. D. Miller, J. Phys. Chem. **98**, 12466 (1994).
[78] R. W. Boyd, *Nonlinear Optics* (Academic, Boston, 1992), p. 36ff.
[79] S. Mukamel, *Principles of Nonlinear Optical Spectroscopy* (Oxford University Press, Oxford, 1995).
[80] Y. R. Shen, *The Principles of Nonlinear Optics* (Wiley, New York, 1984).
[81] R. W. Terhune, P. D. Maker, and C. M. Savage, Phys. Rev. Lett. **14**, 681 (1965).
[82] P. D. Maker, Phys. Rev. A **1**, 923 (1970).
[83] D. Débarre, M. Lefebvre, and M. Péalat, Opt. Commun. **69**, 362 (1989).
[84] R. Trebino and L. A. Rahn, Opt. Lett. **15**, 354 (1990).
[85] A. Tokmakoff, J. Chem. Phys. **105**, 1 (1996).
[86] A. Tokmakoff, J. Chem. Phys. **105**, 13 (1996).
[87] J. T. Fourkas (unpublished).
[88] E. T. J. Nibbering, D. A. Wiersma, and K. Duppen, Chem. Phys. **183**, 167 (1994).
[89] H. Grabert, P. Schramm, and G.-L. Ingold, Phys. Rep. **168**, 115 (1988).
[90] J. T. Fourkas, H. Kawashima, and K. A. Nelson, J. Chem. Phys. **103**, 4393 (1995).
[91] D. W. Oxtoby and S. A. Rice, Chem. Phys. Lett. **42**, 1 (1976).
[92] W. T. Pollard and R. A. Friesner, J. Chem. Phys. **100**, 5054 (1994).
[93] J. S. Bader and B. J. Berne, J. Chem. Phys. **100**, 8359 (1994).
[94] In Ref. 65 it was shown that for a single harmonic mode the fifth-order response can be written as $R^{(5)}(\tau_1,\tau_2)\sim R^{(3)}(\tau_2)[R^{(3)}(\tau_1)+R^{(3)}(\tau_1+\tau_2)]$. However, for multiple modes it is incorrect to write $R^{(5)}_{\rm tot}(\tau_1,\tau_2)\sim R^{(3)}_{\rm tot}(\tau_2)[R^{(3)}_{\rm tot}(\tau_1)+R^{(3)}_{\rm tot}(\tau_1+\tau_2)]$.